A causal Bayesian model to evaluate shoulder pathology effect on glenoid bone mineral density

Pezhman Eghbali[1], Osman Berk Satir[2], Fabio Becce[3], Patrick Goetti[4], Philippe Büchler[2], Dominique P. Pioletti[1], Alexandre Terrier[1,2*]

[1]Laboratory of Biomechanical Orthopedics, Ecole Polytechnique Fédérale de Lausanne, Institute of Bioengineering, Switzerland.
[2]ARTORG Center for Biomedical Engineering Research, University of Bern, Switzerland.
[3]Department of Diagnostic and Interventional Radiology, Lausanne University Hospital and University of Lausanne, Switzerland.
[4]Service of Orthopedics and Traumatology, Lausanne University Hospital and University of Lausanne, Switzerland.

*Corresponding author(s). E-mail(s): alexandre.terrier@epfl.ch;
Contributing authors: pezhman.eghbalishamsabadi@epfl.ch; osman.satir@unibe.ch; Fabio.Becce@chuv.ch; Patrick.Goetti@chuv.ch; philippe.buechler@unibe.ch; dominique.pioletti@epfl.ch;

Abstract

Background: The effect of shoulder pathologies on glenoid bone mineral density (BMD) remains unclear and can be critical in surgical treatments. It is thus useful to predict this effect and understand how it is influenced by sex, age, and body mass index (BMI), in various glenoid locations.
Methods: To address this question, we developed a causal model and used do-calculus to identify the minimal adjustment set of covariate variables and developed a varying-intercept varying-slope Bayesian model. We considered two common shoulder pathologies, primary osteoarthritis (OA) and cuff tear arthropathy (CTA), and compared them with normal shoulders (CTRL). Glenoid BMD was automatically measured on computed tomography scans of 93 OA, 53 CTA, and 133 CTRL subjects.
Results: OA and CTA subjects had higher BMD than CTRL in subchondral trabecular bone. This difference was affected by sex, increased with age, and was

stable with BMI. BMD was higher in OA than CTA, especially on the posterior side.
Conclusion: This causal model estimates the causal effect of pathology BMD, which could be useful for surgery planning, outcome prediction, and understanding of the associated pathophysiology.

Keywords: shoulder pathology, glenoid bone mineral density, causal inference, Bayesian statistics

1 Supplementary materials

1.1 Model validation with synthetic data

To ensure that the proposed model could recover the real parameter values based on the causal structure, we tested the model with synthetic data before feeding it the real data. We fixed the average, age, and BMI (α, β, and γ) effects on glenoid BMD and we generated data stochastically as follows (For simplicity we did not consider the kernel effect here).

$$BMD_i \sim Normal(\mu_i, \sigma) \tag{1}$$

$$\mu_i = \alpha_{l[i],g[i]} + \beta_{l[i],g[i]}(age_i - \overline{\text{age}}) + \gamma_{l[i],g[i]}(BMI_i - \overline{\text{BMI}}) + \epsilon \tag{2}$$

Where ϵ is the noise term, considered to be $Normal(0, 1)$. For a better match of the data generation process with the real data, we considered a similar number of subjects for each group as in the real dataset of the study. The code for this validation is also available in the repository (gitLab). With this process, we also assessed the necessary number of subjects for a reliable estimate of the parameters. We found out that 300 (synthetic) subjects would produce reliable estimates of the parameters (Fig A2, A3, A4). This number of synthetic subjects justified the number of real subjects used in this study. With 300 (synthetic) subjects, the difference of the estimates compared to the real effect was 0 [-0.08, 0.05] with the unit of [z-score of ST BMD] for average effect (α), 0 [-0.01 0.01] [z-score of ST BMD / One unit change of age] for age effect (β), and -0.01 [-0.02, 0.00] [z-score of ST BMD / One unit change of BMI] for BMI effect (γ). We point out that this synthetic data simulation, indeed could not capture everything that may happen in the real dataset, nonetheless, it helped in providing insight into the number of data necessary for the study to have reliable estimates. This analysis was also sensitive to the noise term ϵ. We believe that a $Normal(0, 1)$ noise added to the generated BMD can be a reliable method for evaluating the performance of the model. Increasing/decreasing the noise level obviously decreases/increases the estimate's reliability.

1.2 Likelihood evaluation

For the outcome distribution, we argue that a normal distribution was a suitable choice. We showed this point by plotting the pareto-smoothed importance sampling cross-validation (PSIS) [1] and widely applicable information criteria (WAIC) [2] of the model (Fig. A5). For the normal-based model's out-of-sample predictions, there were no points with higher PSIS Pareto k than 0.7 which could make the importance weight unreliable and WAIC penalty high [1].

1.3 Prior predictive simulation

Predictive prior simulation is assessing what we might see from our set of priors, before introducing real data to the model [3]. This technique could be useful in designing priors to minimize unrealistic predictions. In Stan, we could use the same model definition and just disable the likelihood part of the model. We used this technique to design the priors of the model and evaluated the predicted BMD differences (Fig. A6, A7, A8, A9). The tuned set of the priors resulted in a mainly higher ST BMD for OA than CTRL subjects, with a higher density between 100 to 300 HU (Fig. A6, A8), and a mainly CTA-CTRL difference in the range of -100 to 200 HU (Fig. A7, A9). Moreover, the ST BMD changes with age and BMI also seemed reasonable. There were a few extreme and unrealistic slopes, which was indeed expected as samples could be drawn from tails of the parameters distribution leading to strange predictions.

1.4 More simulations from posterior distribution

Here we provided more simulations with the Bayesian model. We kept age constant at 50, 60, 70, 80, and 90 years old, and at each age, we simulated OA-CTRL and CTA-CTRL ST BMD differences for female and male, at BMI of 17, 25, and 33 (Fig. A13).

1.5 CT Kernel

We assessed the kernel effect on calculated ST BMD differences for OA-CTRL female (Fig. A14). As before we kept all of the variables constant and only changed the kernel. Differences were negligible and the highest difference happened in anterior-superior octant (24.8 [13.1 36.8] HU at 65 years).

1.6 Post stratification

Post-stratification is a statistical technique used to adjust estimates from a sample to better reflect the known distribution of a population. It involves dividing the population into strata (subgroups) based on certain characteristics (e.g., age, sex, or disease status) and reweighting the sample estimates to match the population proportions in each stratum. Mathematically, the post-stratified estimate $\hat{Y}_{ps}$ for a population parameter Y can be expressed as:

$$\hat{Y}_{ps} = \sum_{h=1}^{H} \frac{N_h}{N} \hat{Y}_h,$$

where H is the number of strata, N_h is the population size of stratum h, N is the total population size, and $\hat{Y}_h$ is the sample estimate for stratum h [4]. This approach reduces bias and improves precision by ensuring that the sample reflects the population structure, particularly when certain subgroups are underrepresented in the sample. In our study, post-stratification could be applied to adjust predictions of glenoid BMD across different shoulder conditions (e.g., OA, CTA) and demographic groups, ensuring that our results generalize to the target population. However, a key challenge is that the true population distribution of these shoulder pathologies is not precisely known, which limits our ability to definitively apply post-stratification. Despite this limitation, exploring the potential impact of post-stratification under a range of plausible population proportions provides valuable insights into the sensitivity of our estimates. To explore the impact of post-stratification on our estimates, we applied this technique under several plausible population distributions. Specifically, we tested three scenarios with varying proportions of OA, CTA, and CTRL groups, stratified by sex. In the first scenario, we assumed a population dominated by control groups, with 40% female CTRL and 40% male CTRL, while OA and CTA groups were relatively rare (10% female OA, 5% male OA, 2.5% female CTA, and 2.5% male CTA). In the second scenario, we balanced the proportions, with 35% female CTRL and 35% male CTRL, 10% female OA and 10% male OA, and 5% female CTA and 5% male CTA. In the third scenario, we assumed a higher prevalence of CTA, with 25% female CTRL and 25% male CTRL, 12.5% female OA and 12.5% male OA, and 10% female CTA and 10% male CTA. These scenarios allowed us to assess the sensitivity of our estimates to different assumptions about the population distribution of shoulder pathologies and demographic characteristics. We evaluated the effect of post-stratification on the BMD difference between OA and CTRL while varying age and keeping BMI constant in each of the octants. The differences between the three scenarios were relatively small (Fig. A15). However, the difference between post-stratification and no post-stratification was more pronounced, particularly for males above 70 years of age. This suggests that while the specific population proportions assumed in the post-stratification scenarios had a limited impact on the results, the application of post-stratification itself substantially influenced the estimates, especially in older male subgroups.

1.7 DAG sensitivity analysis

To assess the potential impact of unmeasured confounders on our estimates, we conducted a sensitivity analysis focusing on a hypothetical confounder that acts as a common cause of both shoulder pathology (e.g., OA, CTA) and glenoid BMD. In that case we have to adjust for this confounder in our statistical model as

$$BMD_i \sim Normal(\mu_i, \sigma) \tag{3}$$

$$\mu_i = \alpha_{l[i],g[i]} + \beta_{l[i],g[i]}(age_i - \overline{\text{age}}) + \gamma_{l[i],g[i]}(BMI_i - \overline{\text{BMI}}) + \eta U \tag{4}$$

Here, η represents the effect of the unmeasured confounder U on BMD.

We explored a range of plausible values for η, representing different assumptions about the confounder's influence on BMD. By systematically varying η, we assessed how our estimates of the relationship between shoulder pathology and BMD would be affected. This approach allowed us to quantify the robustness of our findings to unmeasured confounding and to identify conditions under which our conclusions might be significantly impacted.

For instance, when η is assumed to have values of 0.1, 0.2, and 0.6, the simulated difference in BMD corresponding to a -1 z-score versus a $+1$ z-score of U could change by up to an average of 100 HU. These results highlight the potential magnitude of bias introduced by unmeasured confounders (A16).

1.8 HMC Convergence

The trace of the HMC sampling illustrated a robust sampling procedure for all model parameters (Fig A1). The sampling has been performed for 4 chains and 2000 iterations per chain. The initial 50% of the iterations were considered for warm-up and the last 50% for sampling. The trace exhibited characteristics indicative of a sound HMC sampling process: stationary, where the chains remained within the high-probability region of the posterior distribution; mixing, where the chains effectively explored the distribution; and convergence, where multiple chains converged to the same high-probability region.

1.9 Figures

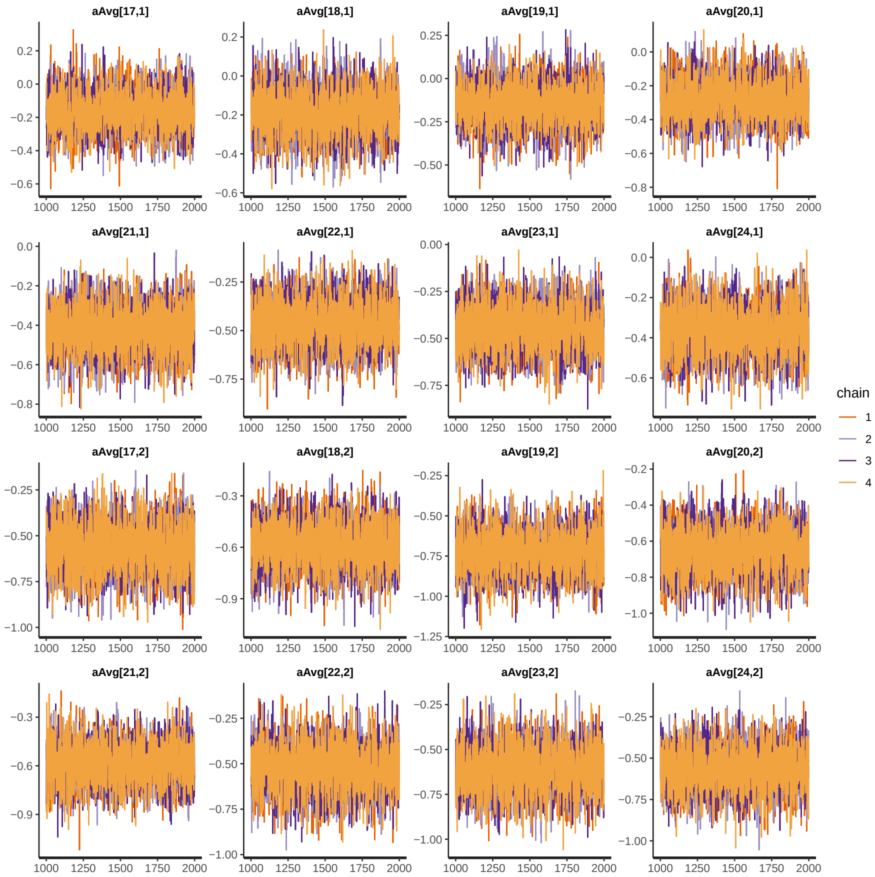
aAvg[17,1]
aAvg[18,1]
aAvg[19,1]
aAvg[20,1]
aAvg[21,1]
aAvg[22,1]
aAvg[23,1]
aAvg[24,1]
aAvg[17,2]
aAvg[18,2]
aAvg[19,2]
aAvg[20,2]
aAvg[21,2]
aAvg[22,2]
aAvg[23,2]
aAvg[24,2]
chain
1
2
3
4

(a)

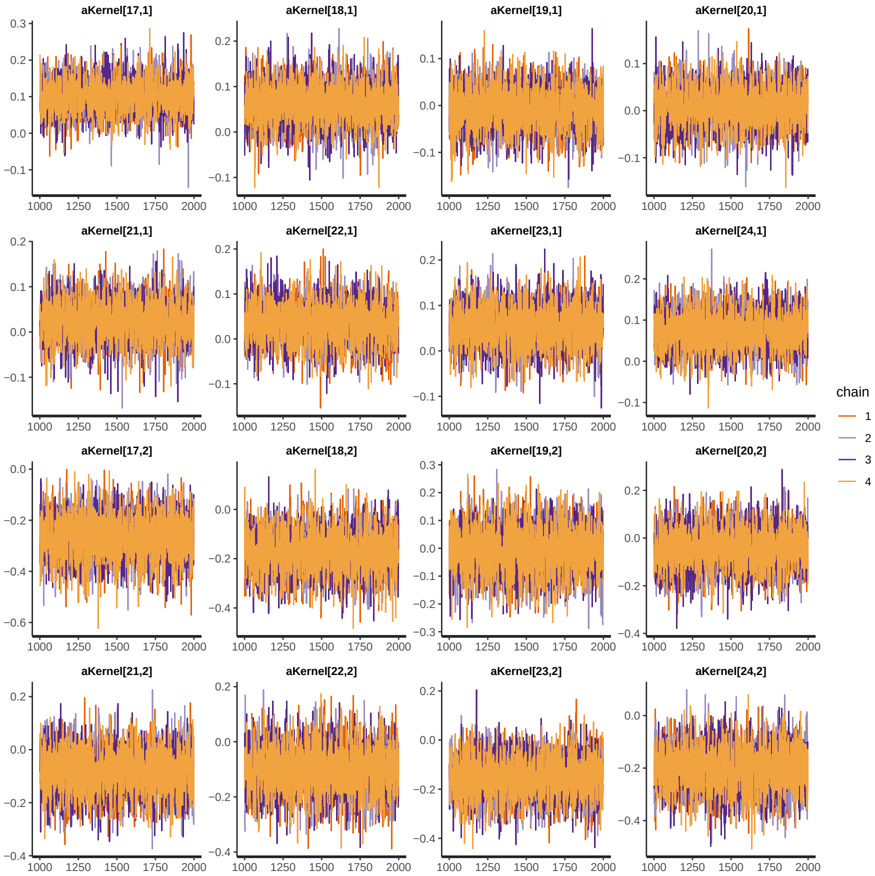
aKernel[17,1]
aKernel[18,1]
aKernel[19,1]
aKernel[20,1]
aKernel[21,1]
aKernel[22,1]
aKernel[23,1]
aKernel[24,1]
aKernel[17,2]
aKernel[18,2]
aKernel[19,2]
aKernel[20,2]
aKernel[21,2]
aKernel[22,2]
aKernel[23,2]
aKernel[24,2]
chain
1
2
3
4
1000
1250
1500
1750
2000

(b)

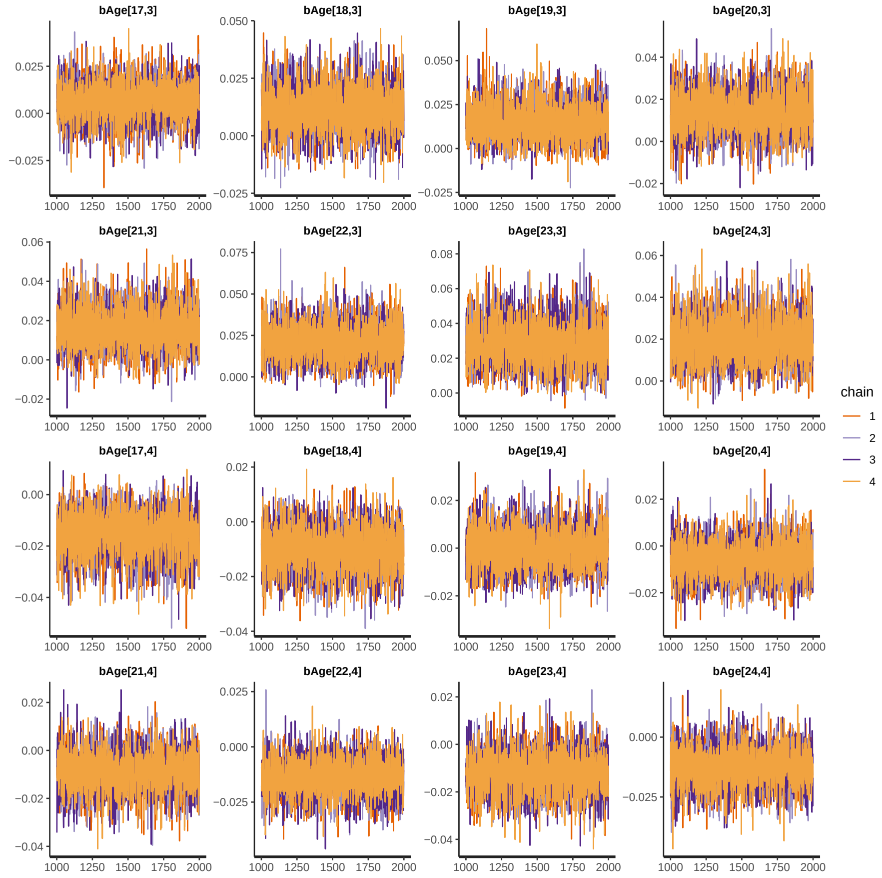
bAge[17,3]
bAge[18,3]
bAge[19,3]
bAge[20,3]
bAge[21,3]
bAge[22,3]
bAge[23,3]
bAge[24,3]
bAge[17,4]
bAge[18,4]
bAge[19,4]
bAge[20,4]
bAge[21,4]
bAge[22,4]
bAge[23,4]
bAge[24,4]
chain
1
2
3
4

(c)

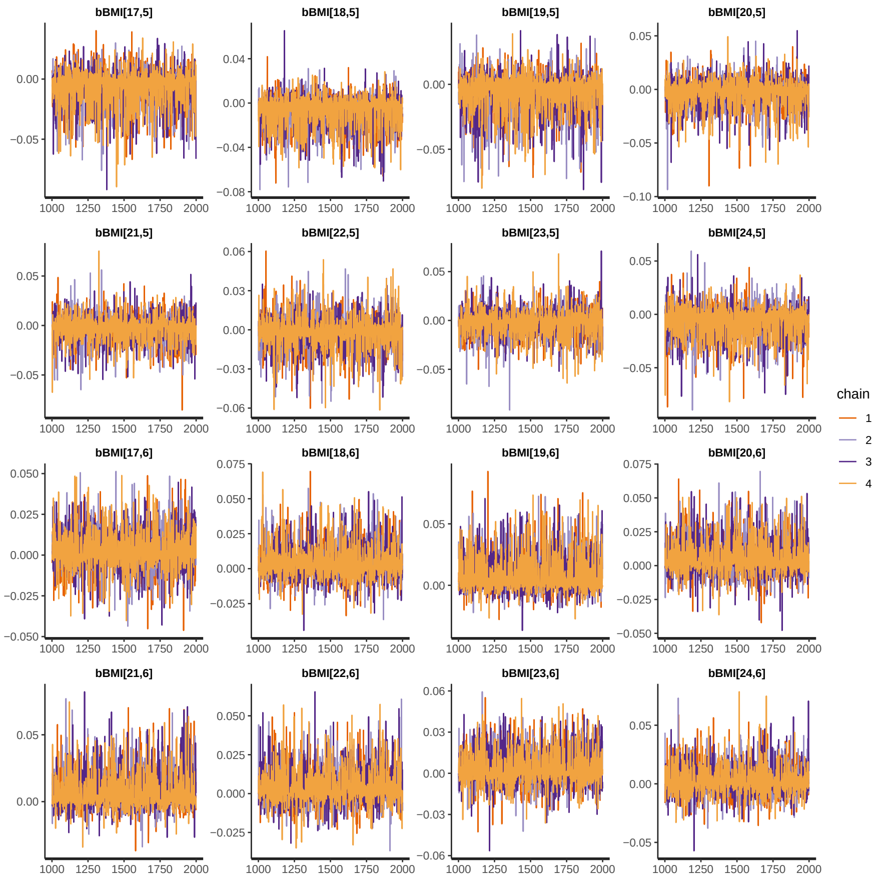

(d)

Fig. A1: Trace of the sampling procedures of the four chains for some of the subsets of (a) α, (b) β, (c) γ, (d) ζ parameters. The x-axis corresponded to iterations of the chains, and the y-axis to the magnitude of the parameters represented as the titles of the graphs.

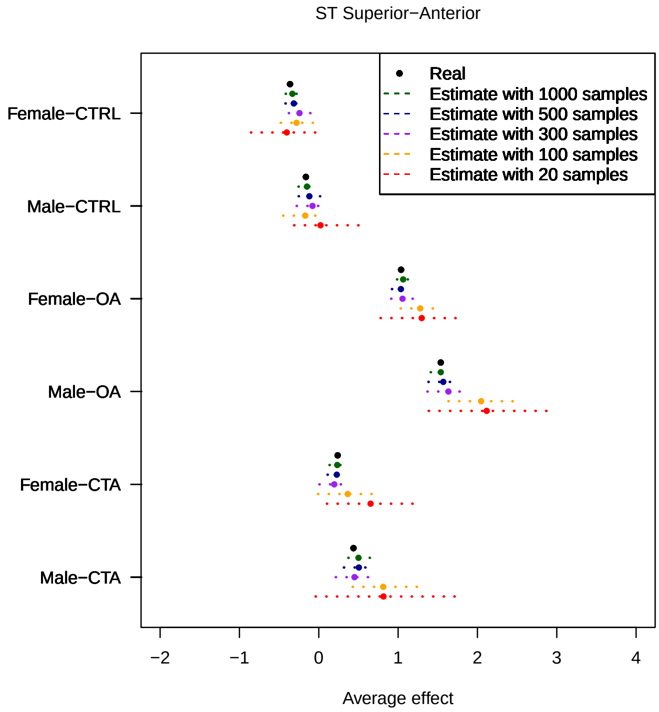
ST Superior−Anterior
Real
Estimate with 1000 samples
Estimate with 500 samples
Estimate with 300 samples
Estimate with 100 samples
Estimate with 20 samples
Female−CTRL
Male−CTRL
Female−OA
Male−OA
Female−CTA
Male−CTA
−2
−1
0
1
2
3
4
Average effect

(a)

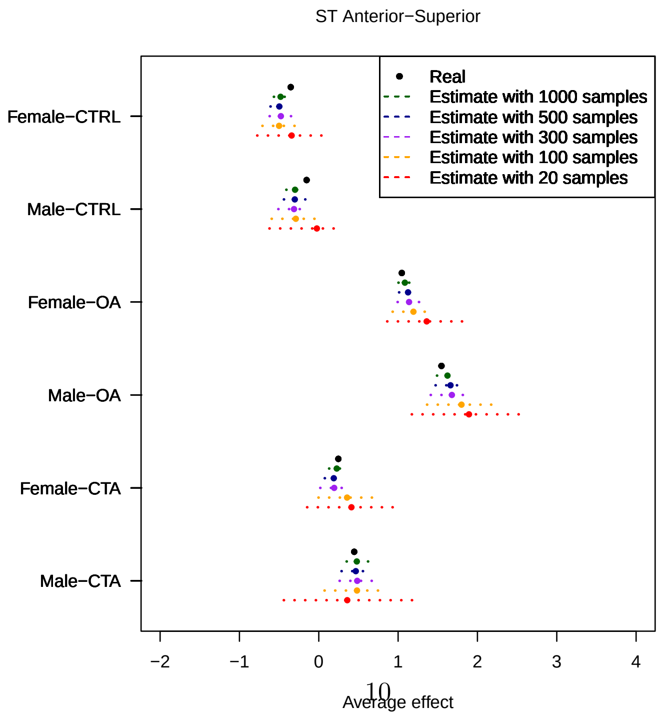
ST Anterior−Superior
Real
Estimate with 1000 samples
Estimate with 500 samples
Estimate with 300 samples
Estimate with 100 samples
Estimate with 20 samples
Female−CTRL
Male−CTRL
Female−OA
Male−OA
Female−CTA
Male−CTA
−2
−1
0
1
2
3
4
Average effect

(b)

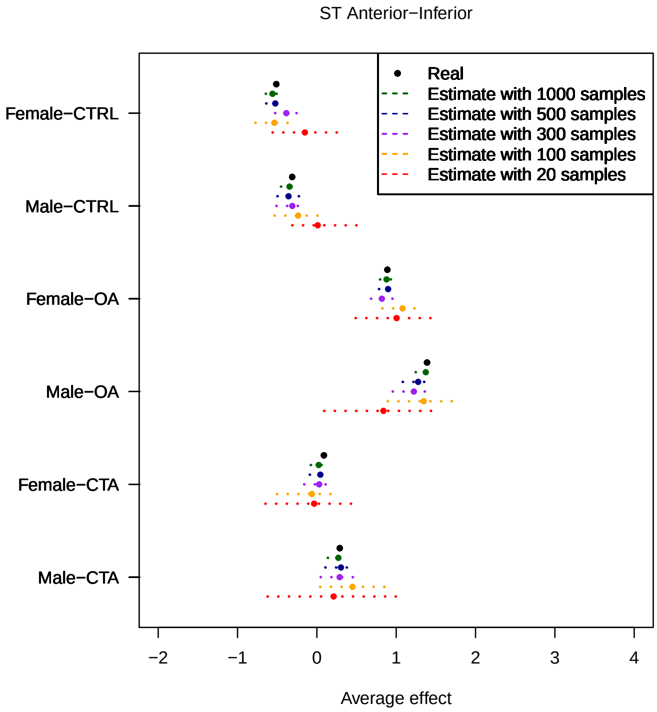
ST Anterior−Inferior
Real
Estimate with 1000 samples
Estimate with 500 samples
Estimate with 300 samples
Estimate with 100 samples
Estimate with 20 samples
Female−CTRL
Male−CTRL
Female−OA
Male−OA
Female−CTA
Male−CTA
−2
−1
0
1
2
3
4
Average effect

(c)

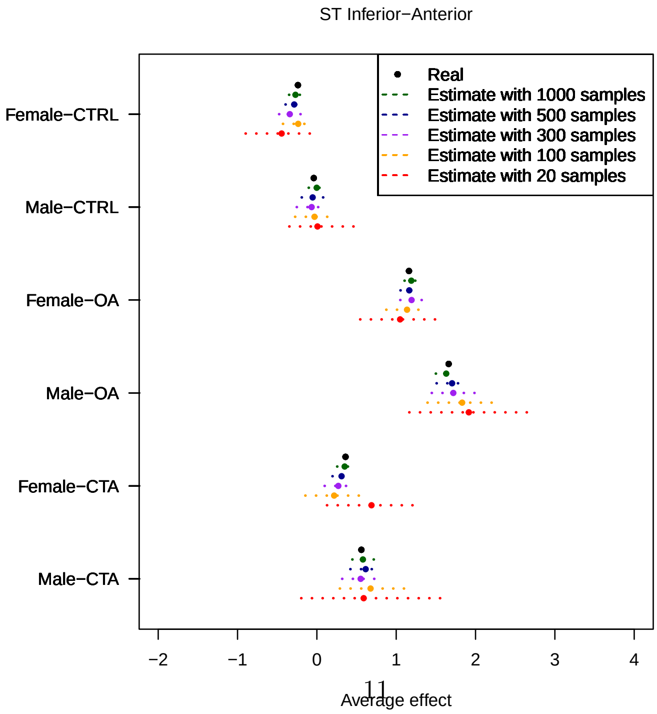
ST Inferior−Anterior
Real
Estimate with 1000 samples
Estimate with 500 samples
Estimate with 300 samples
Estimate with 100 samples
Estimate with 20 samples
Female−CTRL
Male−CTRL
Female−OA
Male−OA
Female−CTA
Male−CTA
−2
−1
0
1
2
3
4
Average effect

(d)

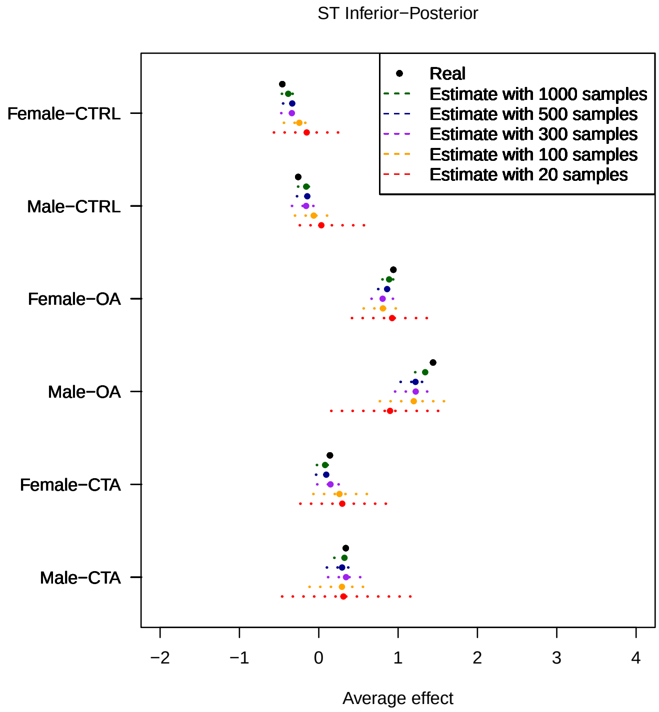
ST Inferior−Posterior
Real
Estimate with 1000 samples
Estimate with 500 samples
Estimate with 300 samples
Estimate with 100 samples
Estimate with 20 samples
Female−CTRL
Male−CTRL
Female−OA
Male−OA
Female−CTA
Male−CTA
−2
−1
0
1
2
3
4
Average effect

(e)

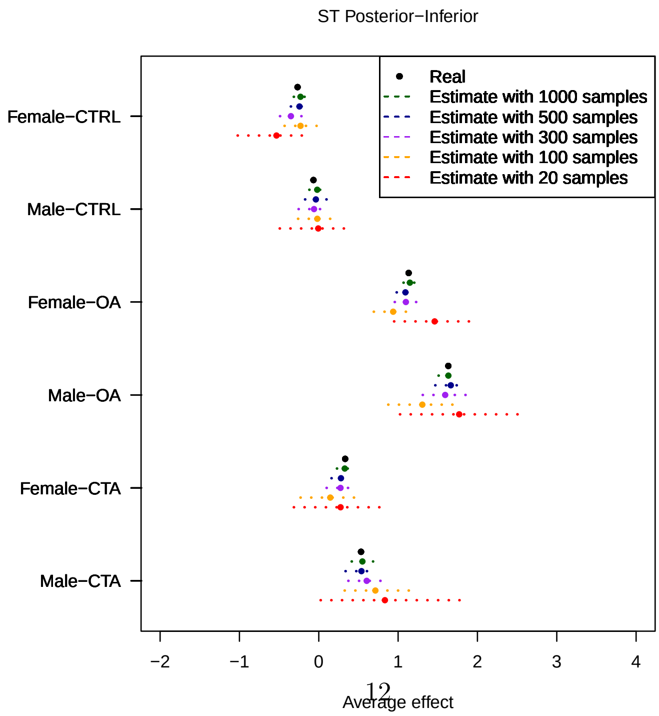
ST Posterior−Inferior
Real
Estimate with 1000 samples
Estimate with 500 samples
Estimate with 300 samples
Estimate with 100 samples
Estimate with 20 samples
Female−CTRL
Male−CTRL
Female−OA
Male−OA
Female−CTA
Male−CTA
−2
−1
0
1
2
3
4
Average effect

(f)

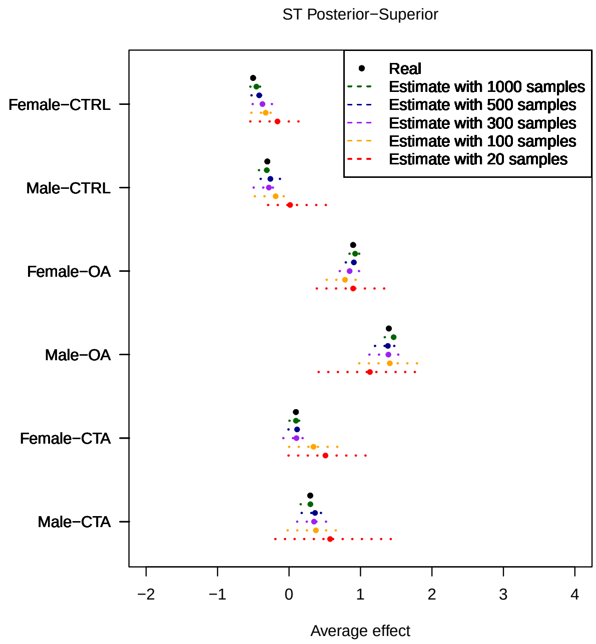

(g)

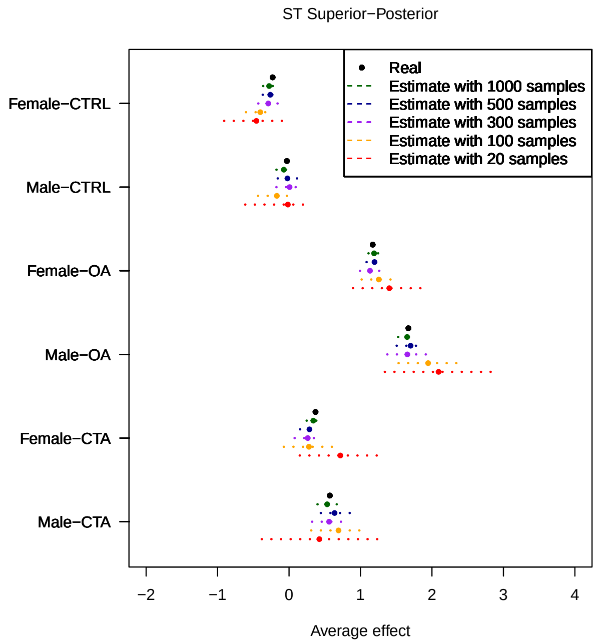

(h)

Fig. A2: Real and estimated values of the average effect of location and group ($\alpha_{l,g}$ in Eq. 4) based on 1000, 500, 300, 100, and 20 synthetic subjects, for each octant, from superior-anterior (a) to superior-posterior (h) of the ST VOI.

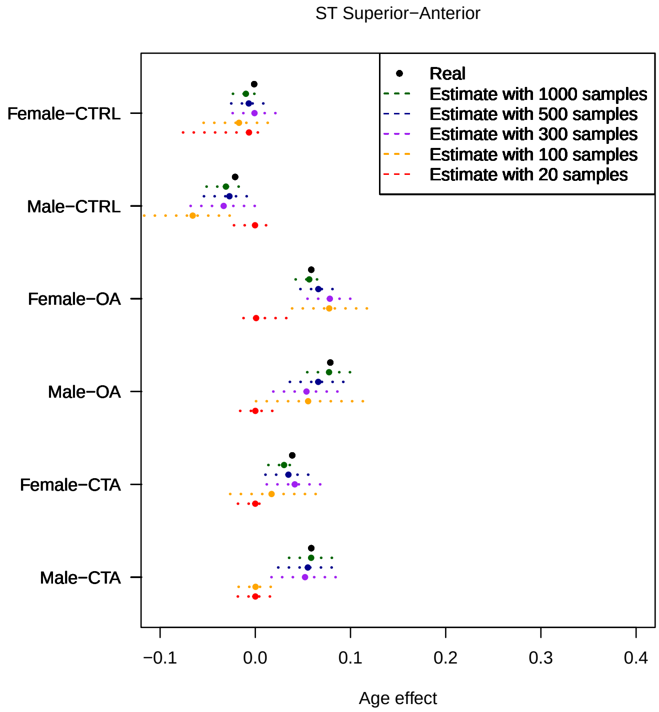

ST Superior−Anterior
Real
Estimate with 1000 samples
Estimate with 500 samples
Estimate with 300 samples
Estimate with 100 samples
Estimate with 20 samples
Female−CTRL
Male−CTRL
Female−OA
Male−OA
Female−CTA
Male−CTA
−0.1
0.0
0.1
0.2
0.3
0.4
Age effect

(a)

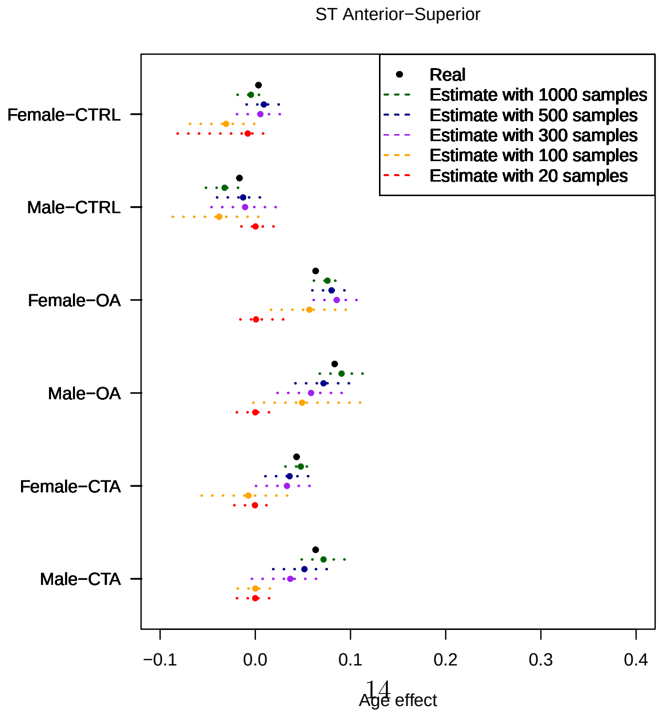

ST Anterior−Superior
Real
Estimate with 1000 samples
Estimate with 500 samples
Estimate with 300 samples
Estimate with 100 samples
Estimate with 20 samples
Female−CTRL
Male−CTRL
Female−OA
Male−OA
Female−CTA
Male−CTA
−0.1
0.0
0.1
0.2
0.3
0.4
Age effect

(b)

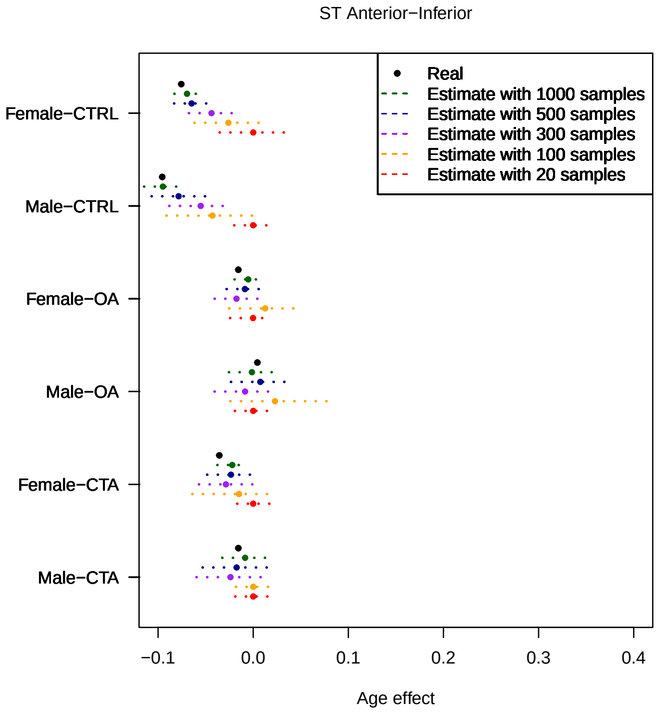
ST Anterior−Inferior
Real
Estimate with 1000 samples
Estimate with 500 samples
Estimate with 300 samples
Estimate with 100 samples
Estimate with 20 samples
Female−CTRL
Male−CTRL
Female−OA
Male−OA
Female−CTA
Male−CTA
−0.1
0.0
0.1
0.2
0.3
0.4
Age effect

(c)

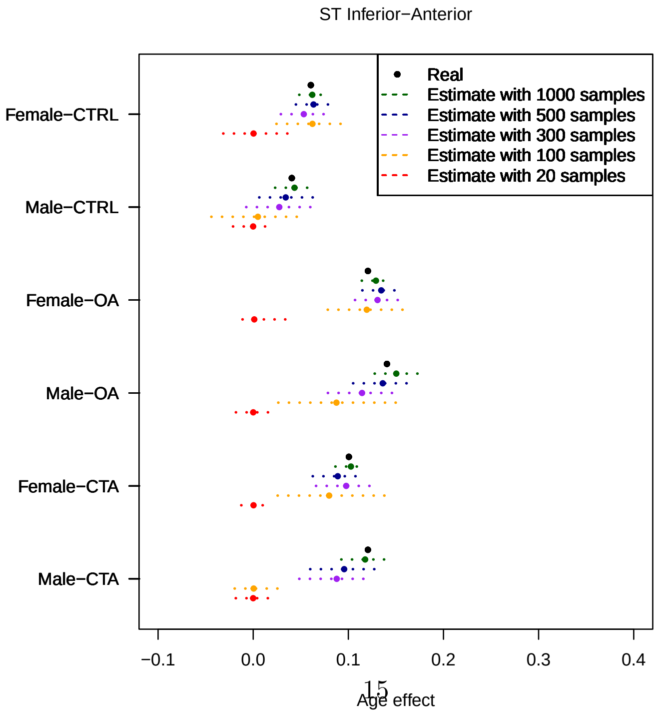
ST Inferior−Anterior
Real
Estimate with 1000 samples
Estimate with 500 samples
Estimate with 300 samples
Estimate with 100 samples
Estimate with 20 samples
Female−CTRL
Male−CTRL
Female−OA
Male−OA
Female−CTA
Male−CTA
−0.1
0.0
0.1
0.2
0.3
0.4
Age effect

(d)

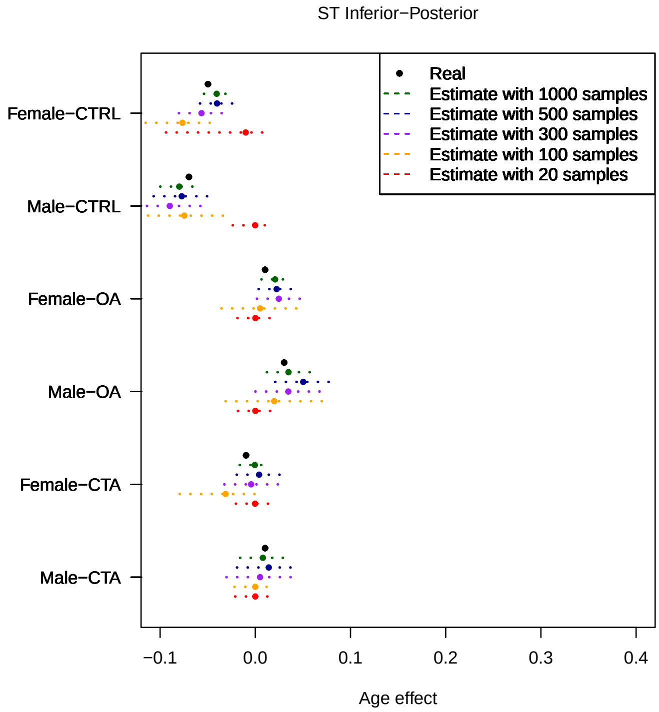
ST Inferior−Posterior
Real
Estimate with 1000 samples
Estimate with 500 samples
Estimate with 300 samples
Estimate with 100 samples
Estimate with 20 samples
Female−CTRL
Male−CTRL
Female−OA
Male−OA
Female−CTA
Male−CTA
−0.1
0.0
0.1
0.2
0.3
0.4
Age effect

(e)

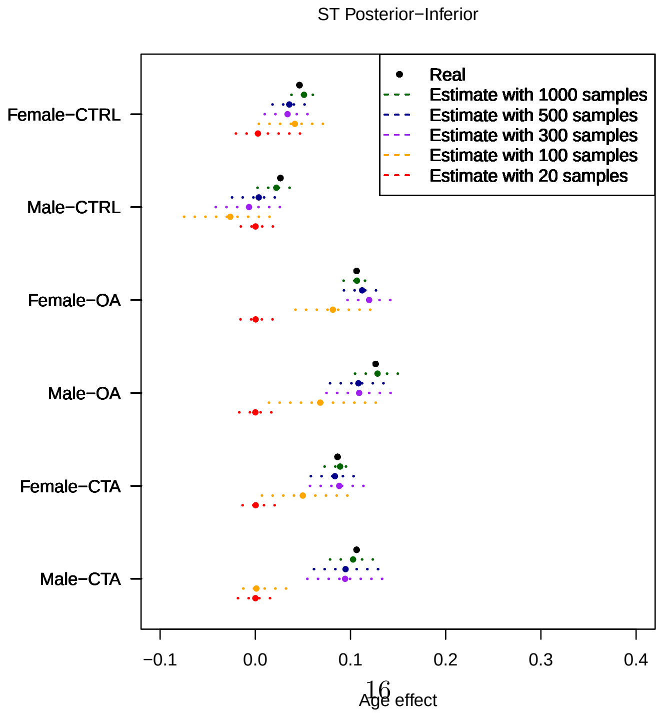
ST Posterior−Inferior
Real
Estimate with 1000 samples
Estimate with 500 samples
Estimate with 300 samples
Estimate with 100 samples
Estimate with 20 samples
Female−CTRL
Male−CTRL
Female−OA
Male−OA
Female−CTA
Male−CTA
−0.1
0.0
0.1
0.2
0.3
0.4
Age effect

(f)

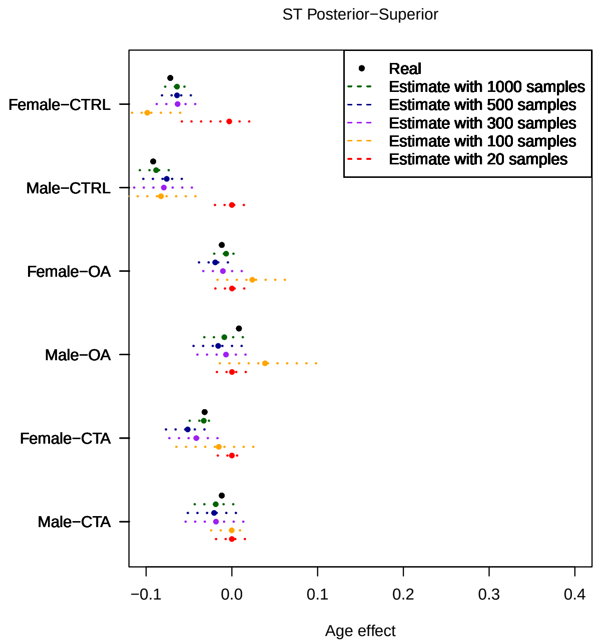

(g)

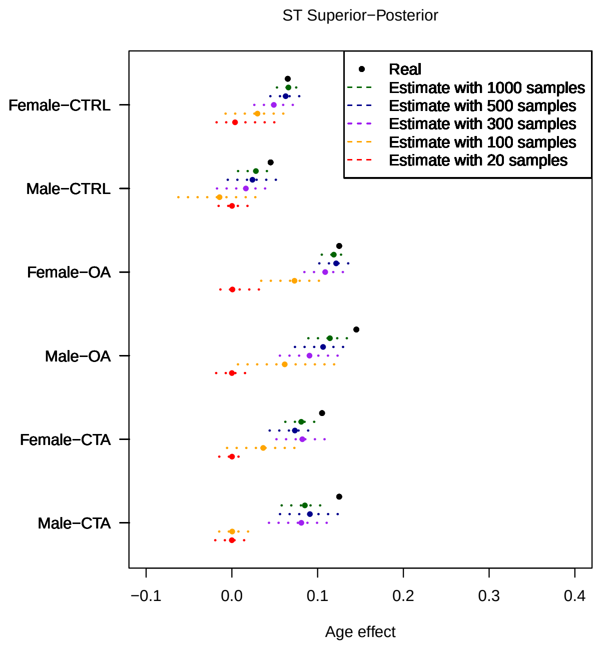

(h)

Fig. A3: Real and estimated values of the age effect of location and group ($\beta_{l,g}$ in Eq. 4) based on 1000, 500, 300, 100, and 20 synthetic subjects, for each octant, from superior-anterior (a) to superior-posterior (h) of the ST VOI.

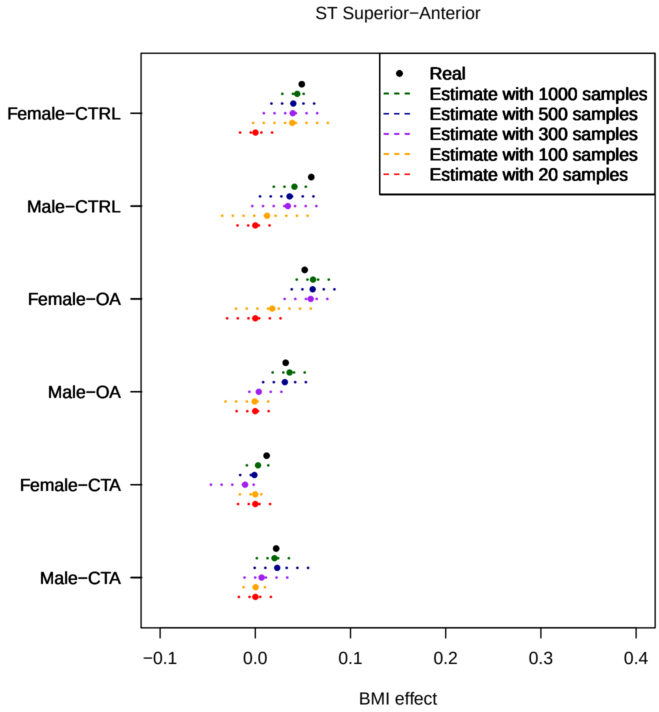
ST Superior−Anterior
Real
Estimate with 1000 samples
Estimate with 500 samples
Estimate with 300 samples
Estimate with 100 samples
Estimate with 20 samples
Female−CTRL
Male−CTRL
Female−OA
Male−OA
Female−CTA
Male−CTA
−0.1
0.0
0.1
0.2
0.3
0.4
BMI effect

(a)

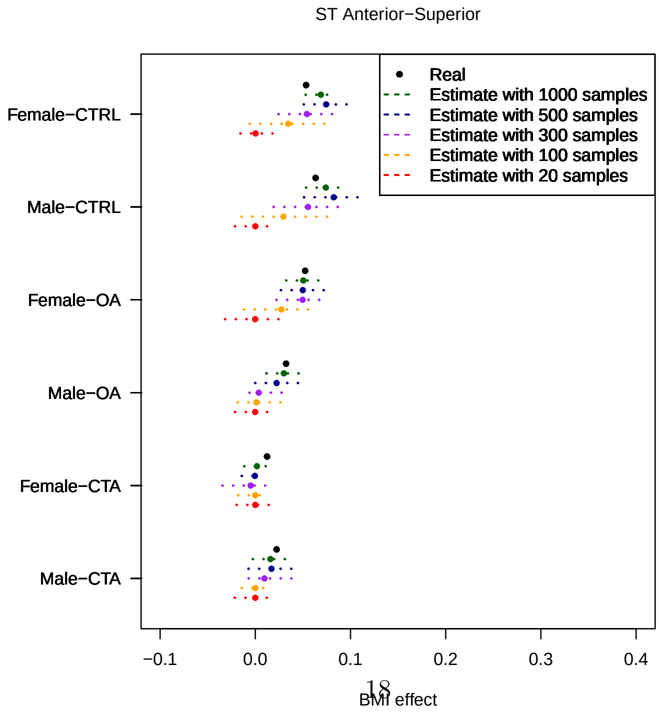
ST Anterior−Superior
Real
Estimate with 1000 samples
Estimate with 500 samples
Estimate with 300 samples
Estimate with 100 samples
Estimate with 20 samples
Female−CTRL
Male−CTRL
Female−OA
Male−OA
Female−CTA
Male−CTA
−0.1
0.0
0.1
0.2
0.3
0.4
BMI effect

(b)

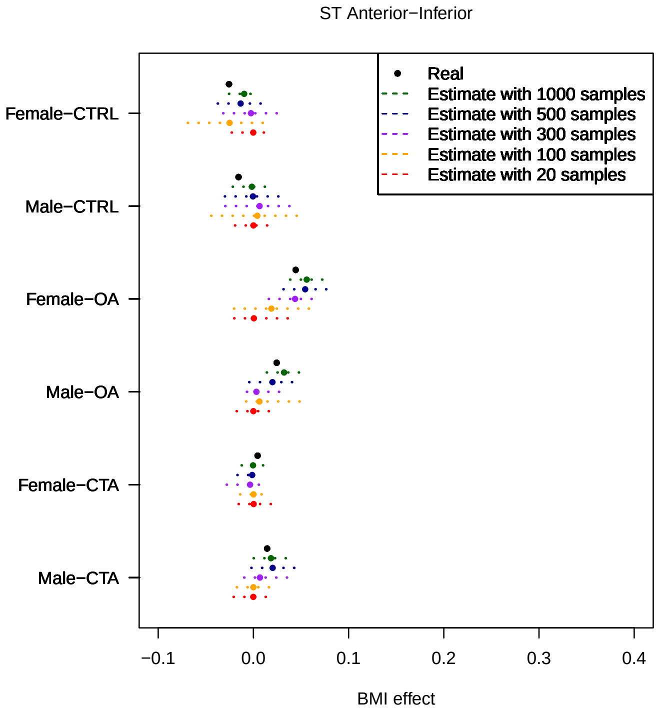
ST Anterior−Inferior
Real
Estimate with 1000 samples
Estimate with 500 samples
Estimate with 300 samples
Estimate with 100 samples
Estimate with 20 samples
Female−CTRL
Male−CTRL
Female−OA
Male−OA
Female−CTA
Male−CTA
−0.1
0.0
0.1
0.2
0.3
0.4
BMI effect

(c)

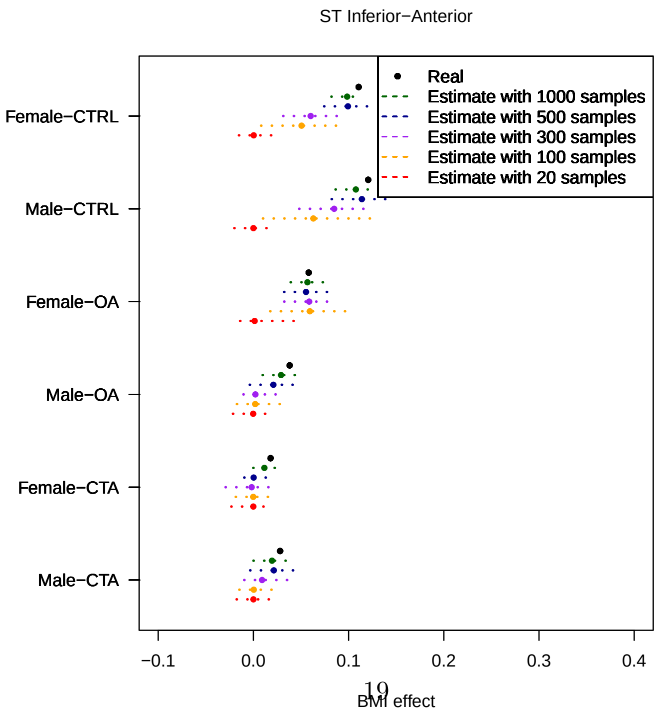
ST Inferior−Anterior
Real
Estimate with 1000 samples
Estimate with 500 samples
Estimate with 300 samples
Estimate with 100 samples
Estimate with 20 samples
Female−CTRL
Male−CTRL
Female−OA
Male−OA
Female−CTA
Male−CTA
−0.1
0.0
0.1
0.2
0.3
0.4
BMI effect

(d)

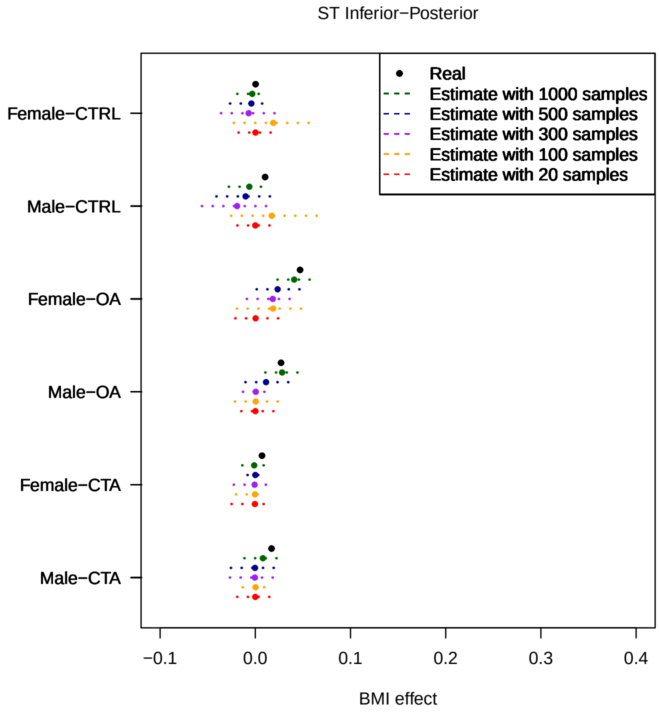
ST Inferior−Posterior
Real
Estimate with 1000 samples
Estimate with 500 samples
Estimate with 300 samples
Estimate with 100 samples
Estimate with 20 samples
Female−CTRL
Male−CTRL
Female−OA
Male−OA
Female−CTA
Male−CTA
−0.1
0.0
0.1
0.2
0.3
0.4
BMI effect

(e)

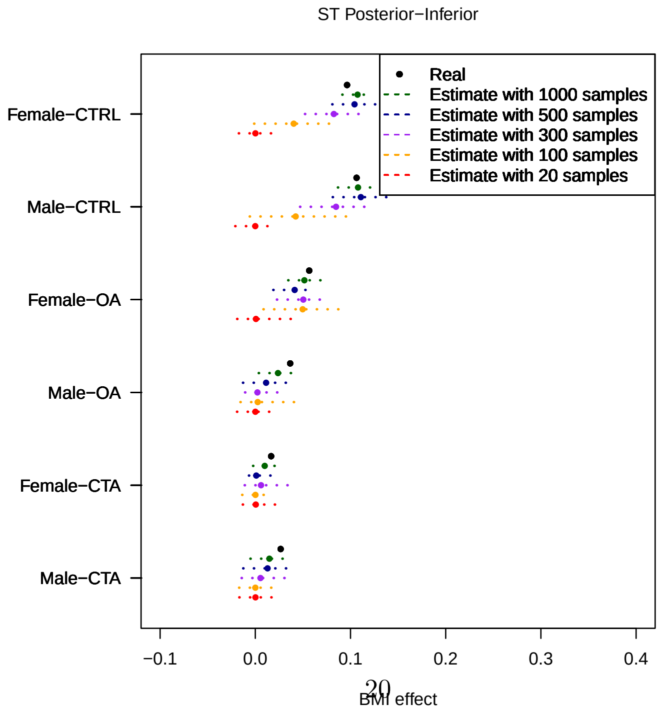
ST Posterior−Inferior
Real
Estimate with 1000 samples
Estimate with 500 samples
Estimate with 300 samples
Estimate with 100 samples
Estimate with 20 samples
Female−CTRL
Male−CTRL
Female−OA
Male−OA
Female−CTA
Male−CTA
−0.1
0.0
0.1
0.2
0.3
0.4
BMI effect

(f)

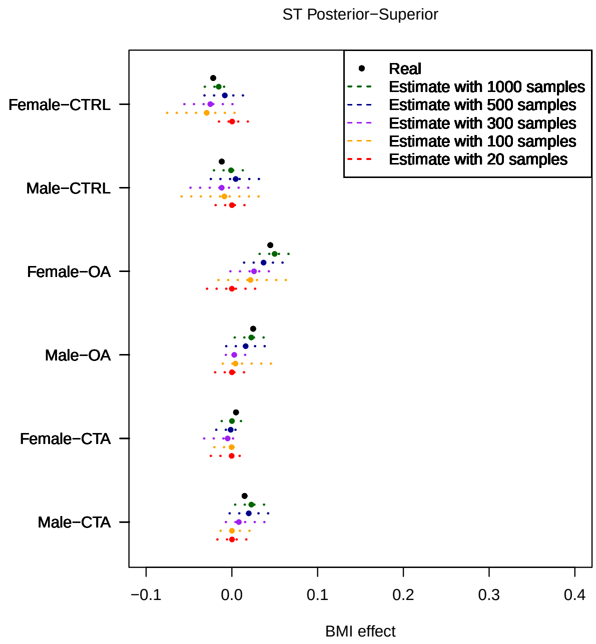

(g)

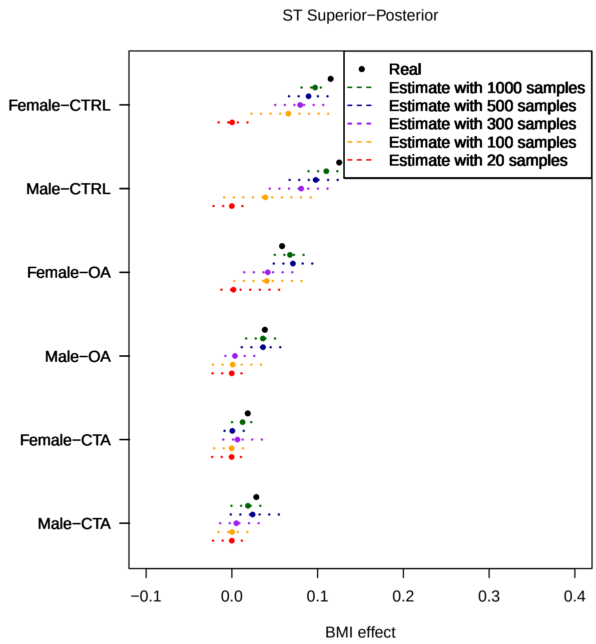

(h)

Fig. A4: Real and estimated values of the BMI effect of location and group ($\gamma_{l,g}$ in Eq. 4) based on 1000, 500, 300, 100, and 20 synthetic subjects, for each octant, from superior-anterior (a) to superior-posterior (h) of the ST VOI.

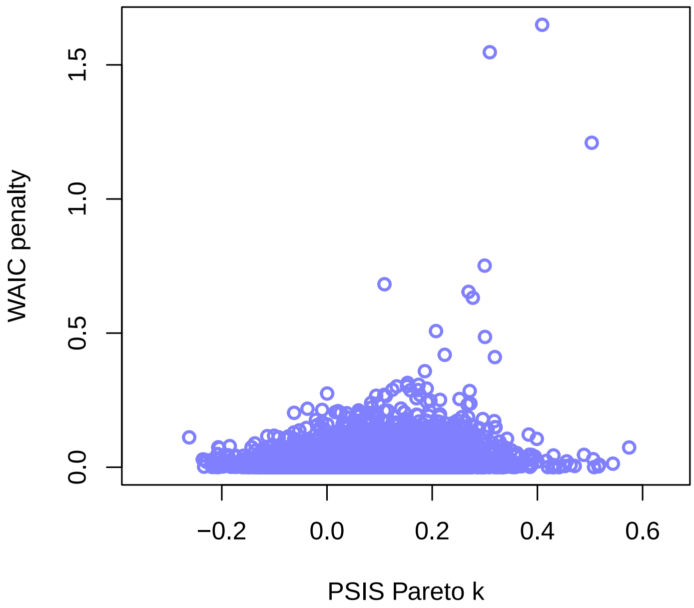

Fig. A5: The pareto k from pareto-smoothed importance sampling cross-validation (PSIS) and widely applicable information criteria (WAIC) for the model with normal distribution as the outcome.

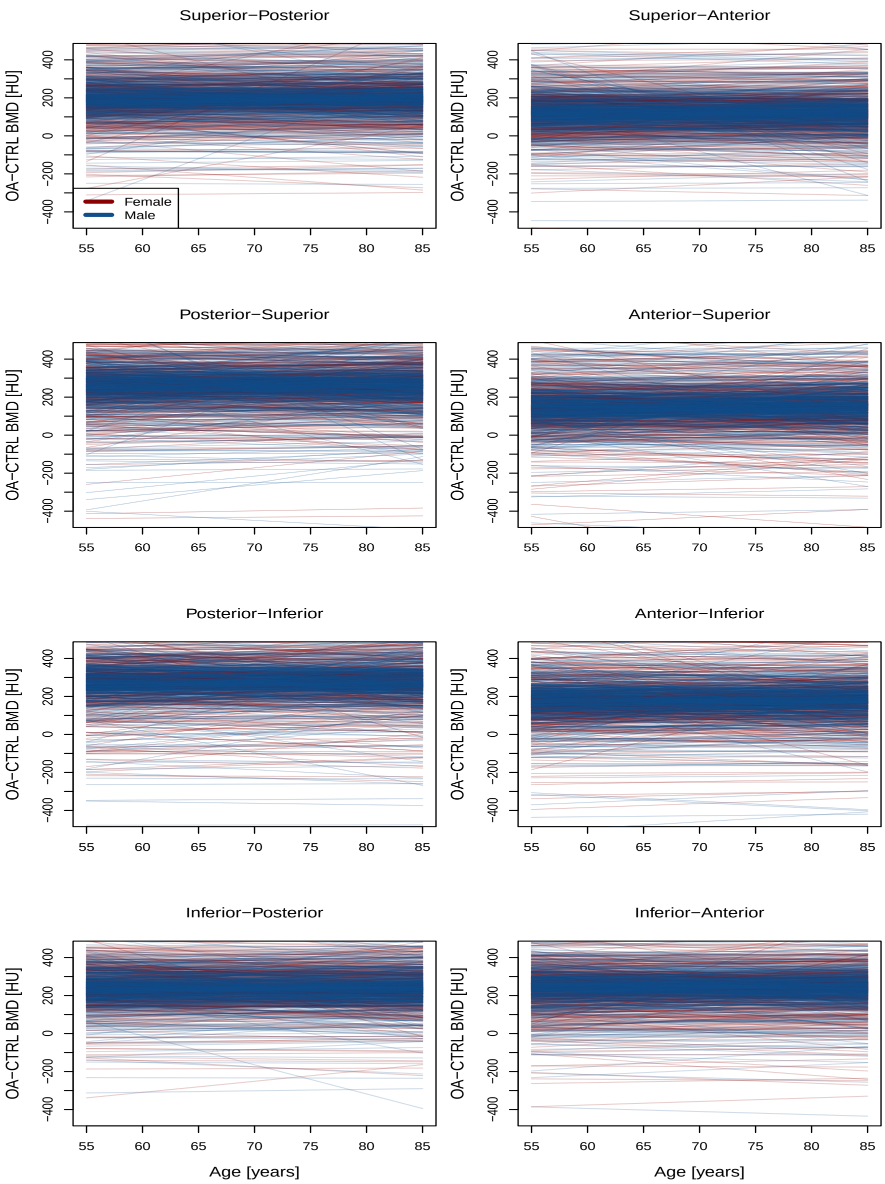

Fig. A6: Prior predictive distribution of difference of BMD in ST between OA and CTRL (vertical axis) vs age (horizontal axis), for male and female, and for the 8 locations, while keeping BMI at 25 kg/m^2.

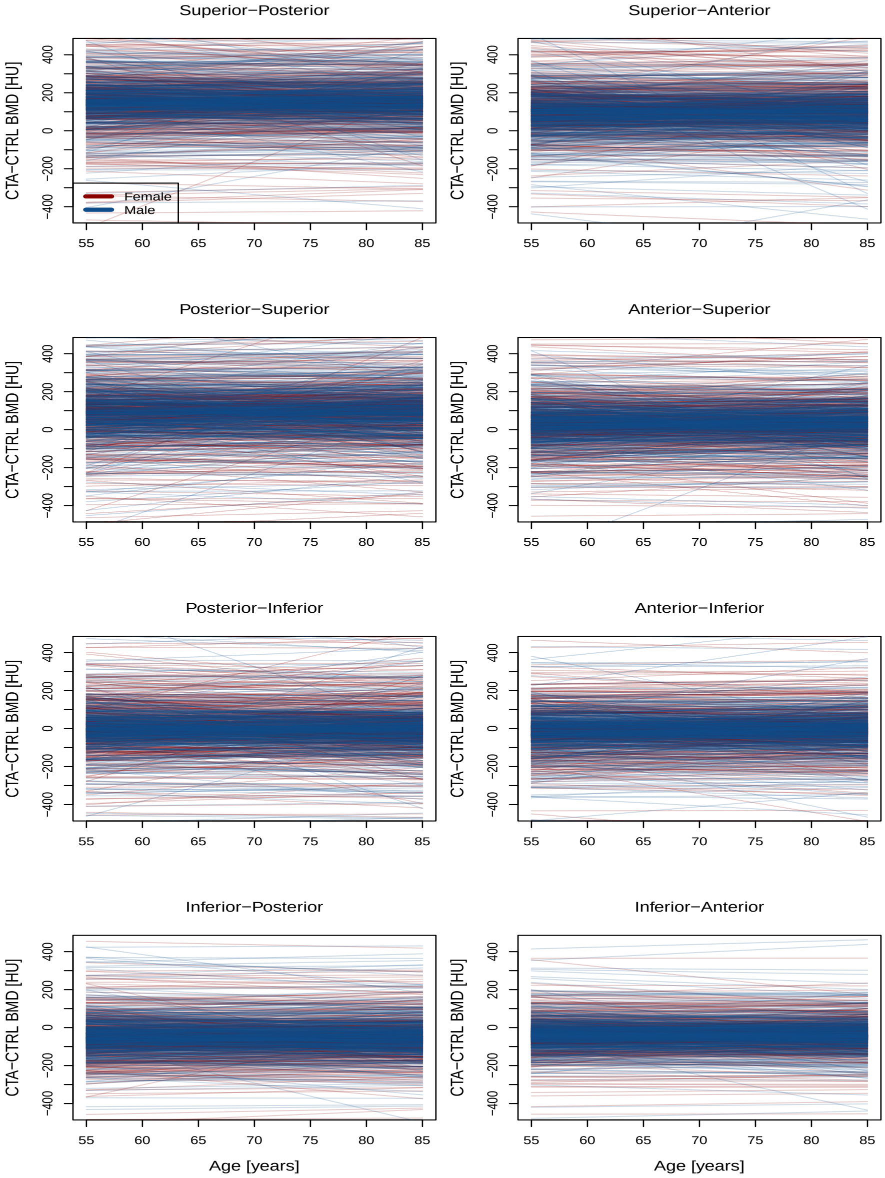

Fig. A7: Prior predictive distribution of difference of BMD in ST between CTA and CTRL (vertical axis) vs age (horizontal axis), for male and female, and for the 8 locations, while keeping BMI at 25 kg/m^2.

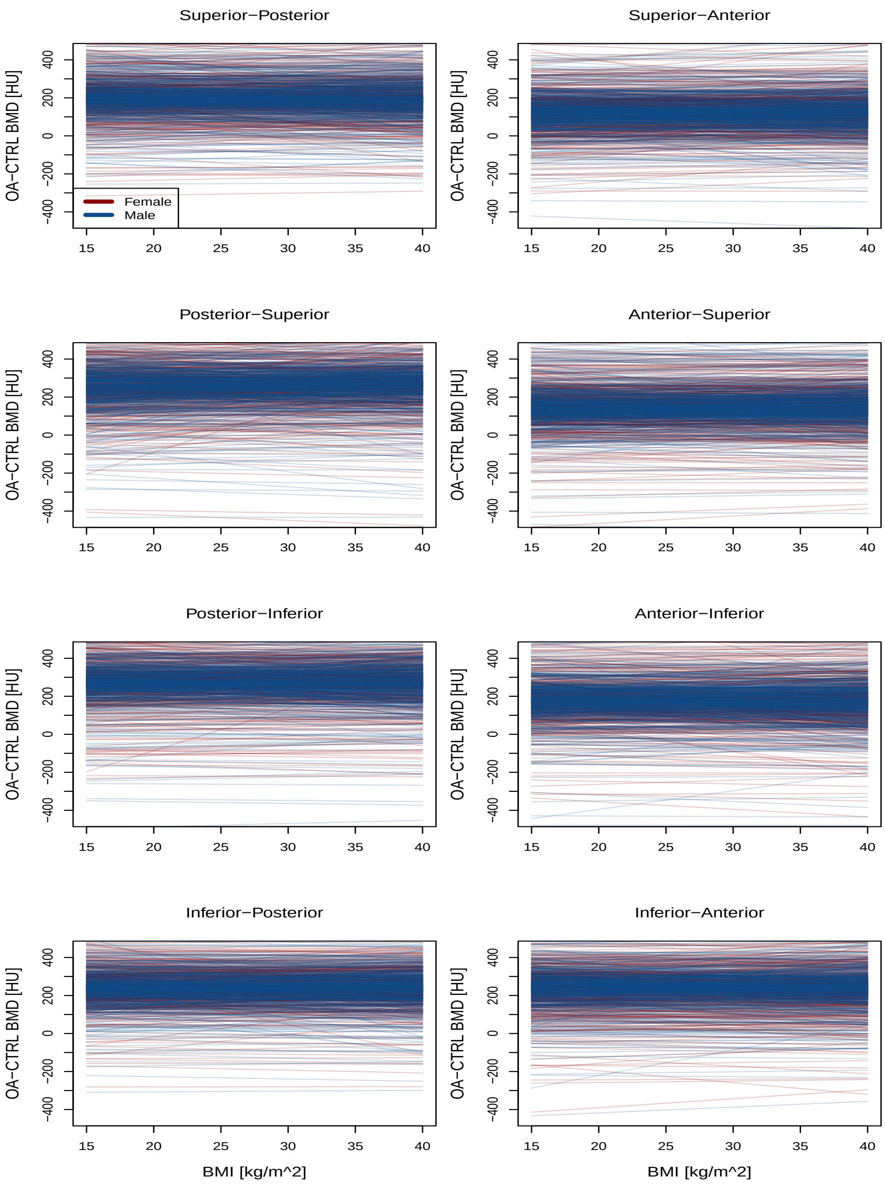

Fig. A8: Prior predictive distribution of difference of BMD in ST between OA and CTRL (vertical axis) vs BMI (horizontal axis), for male and female, and for the 8 locations, while keeping age at 65 years.

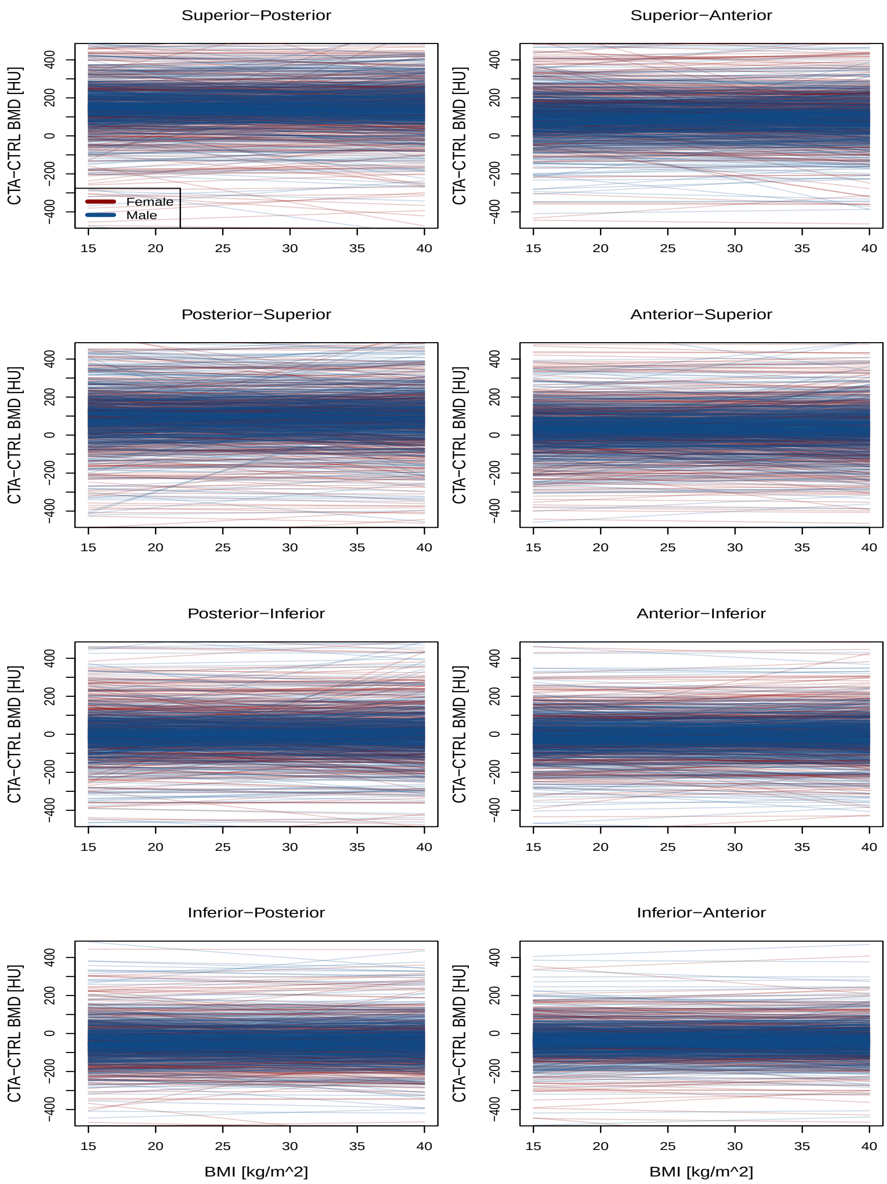

Fig. A9: Prior predictive distribution of difference of BMD in ST between CTA and CTRL (vertical axis) vs BMI (horizontal axis), for male and female, and for the 8 locations, while keeping age at 65 years.

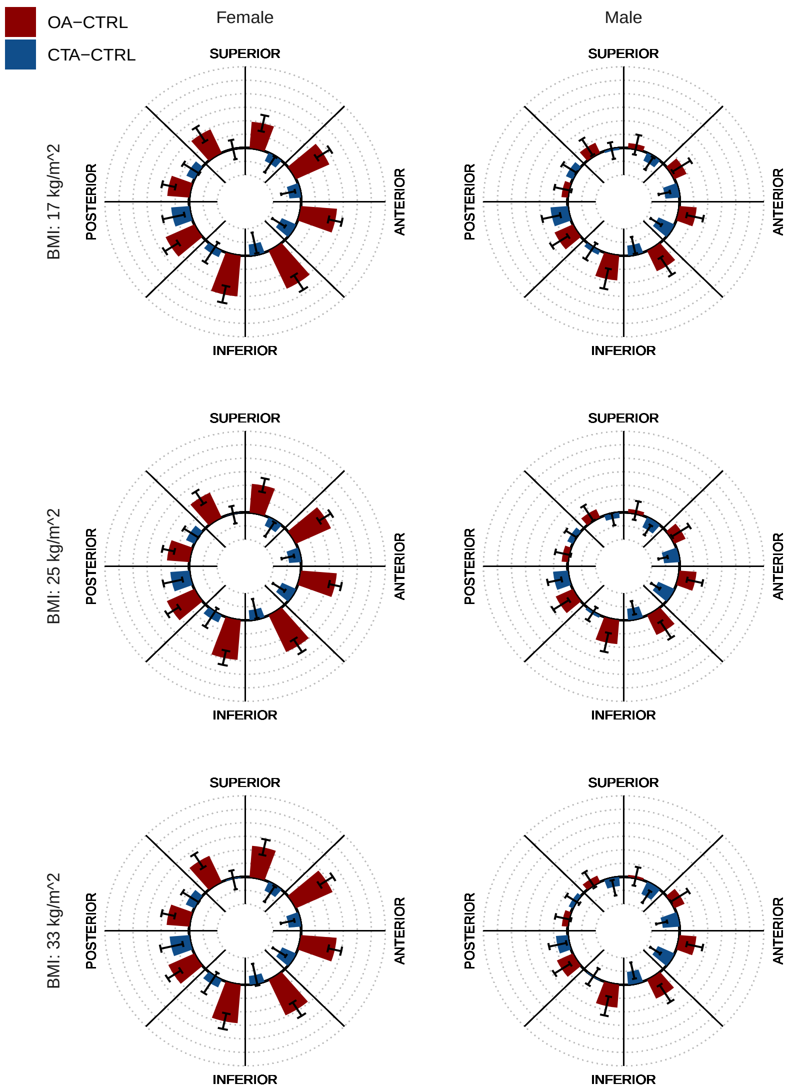
OA−CTRL
CTA−CTRL
Female
Male
BMI: 17 kg/m^2
BMI: 25 kg/m^2
BMI: 33 kg/m^2
SUPERIOR
INFERIOR
POSTERIOR
ANTERIOR

(a)

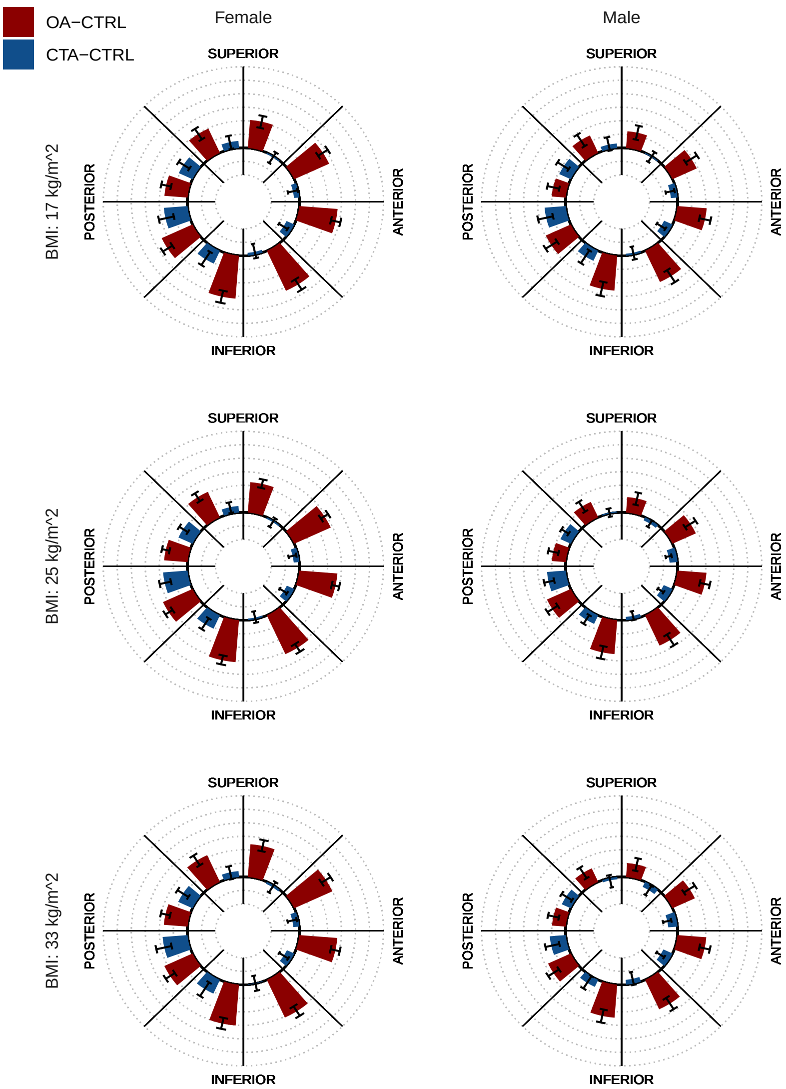
OA−CTRL
CTA−CTRL
Female
Male
BMI: 17 kg/m^2
BMI: 25 kg/m^2
BMI: 33 kg/m^2
SUPERIOR
INFERIOR
POSTERIOR
ANTERIOR

(a)

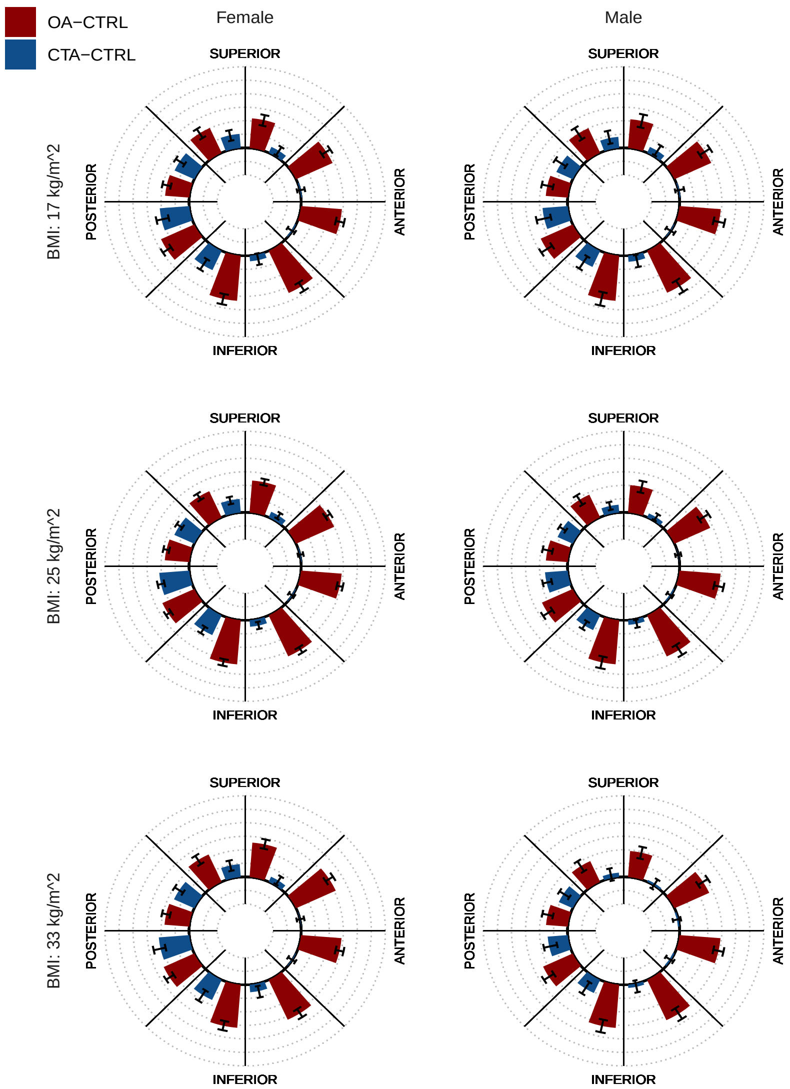
OA−CTRL
CTA−CTRL
Female
Male
BMI: 17 kg/m^2
BMI: 25 kg/m^2
BMI: 33 kg/m^2
SUPERIOR
INFERIOR
ANTERIOR
POSTERIOR

(a)

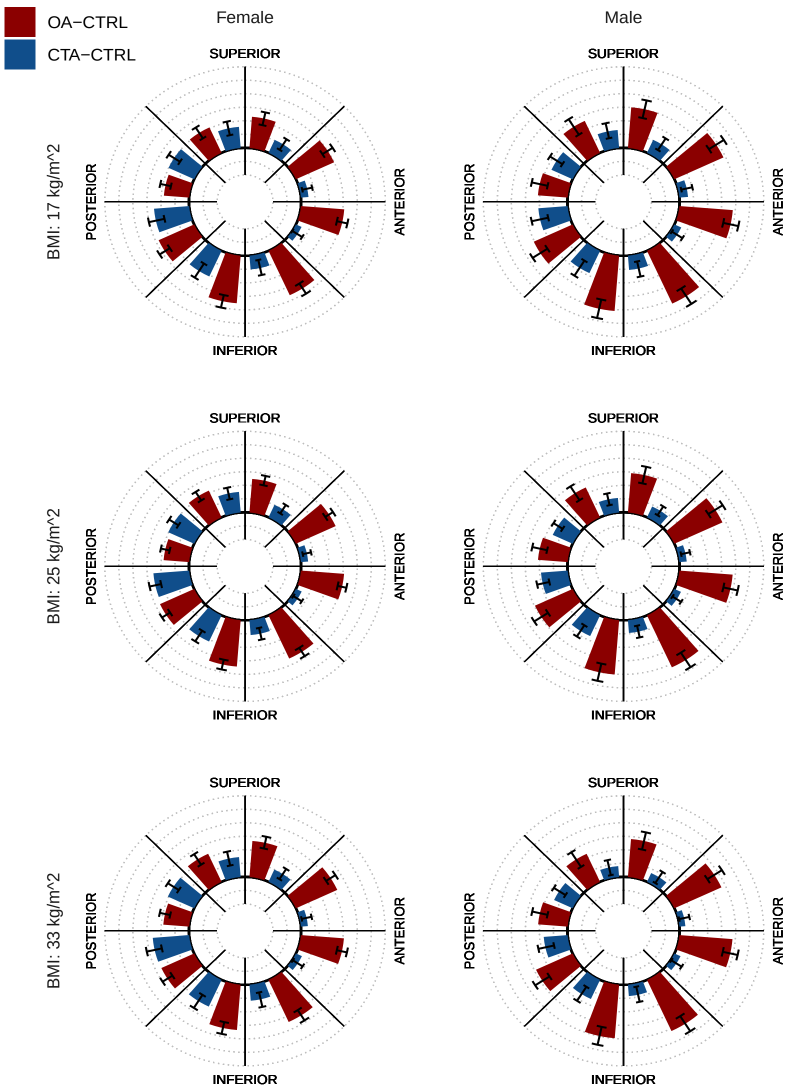
OA−CTRL
CTA−CTRL
Female
Male
BMI: 17 kg/m^2
BMI: 25 kg/m^2
BMI: 33 kg/m^2
SUPERIOR
INFERIOR
POSTERIOR
ANTERIOR

(a)

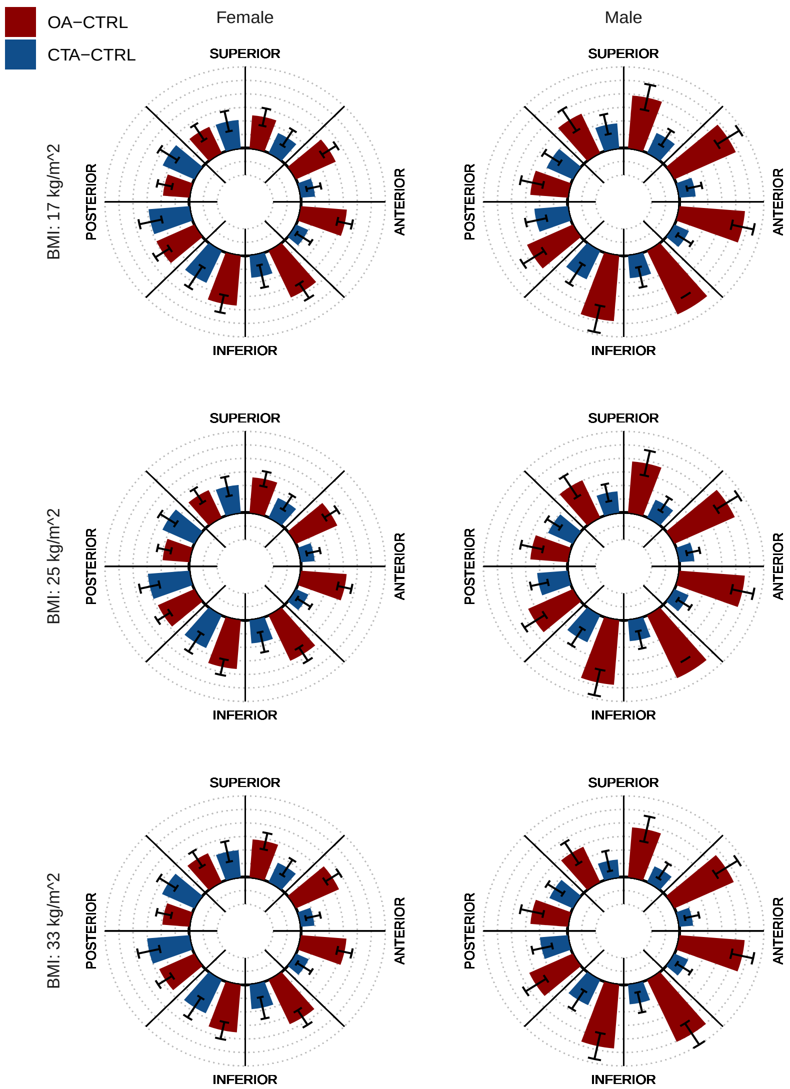

(b)

Fig. A13: Difference and 89% compatibility interval(errorbar) of BMD in ST between pathological and CTR, for male and female at BMIs 17, 25, and 33 kg/m^2 while keeping age at (a) 50 (b) 60 (c) 70 (d) 80 (e) 90 years. The solid circle corresponds to 0 HU and the interval between the concentric circles corresponds to 100 HU.

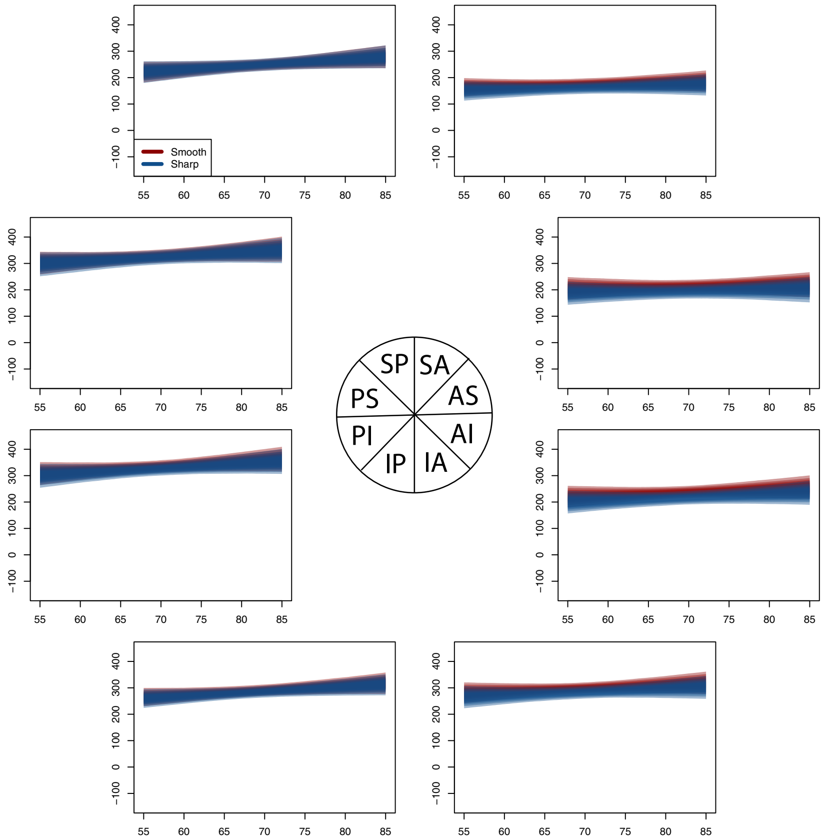

Fig. A14: Difference of BMD in ST between female OA and CTRL (vertical axis) vs age (horizontal axis), while keeping BMI at 25 kg/m^2, for sharp and smooth kernels, and for the 8 locations. The colored surface corresponds to the 89% compatibility interval.

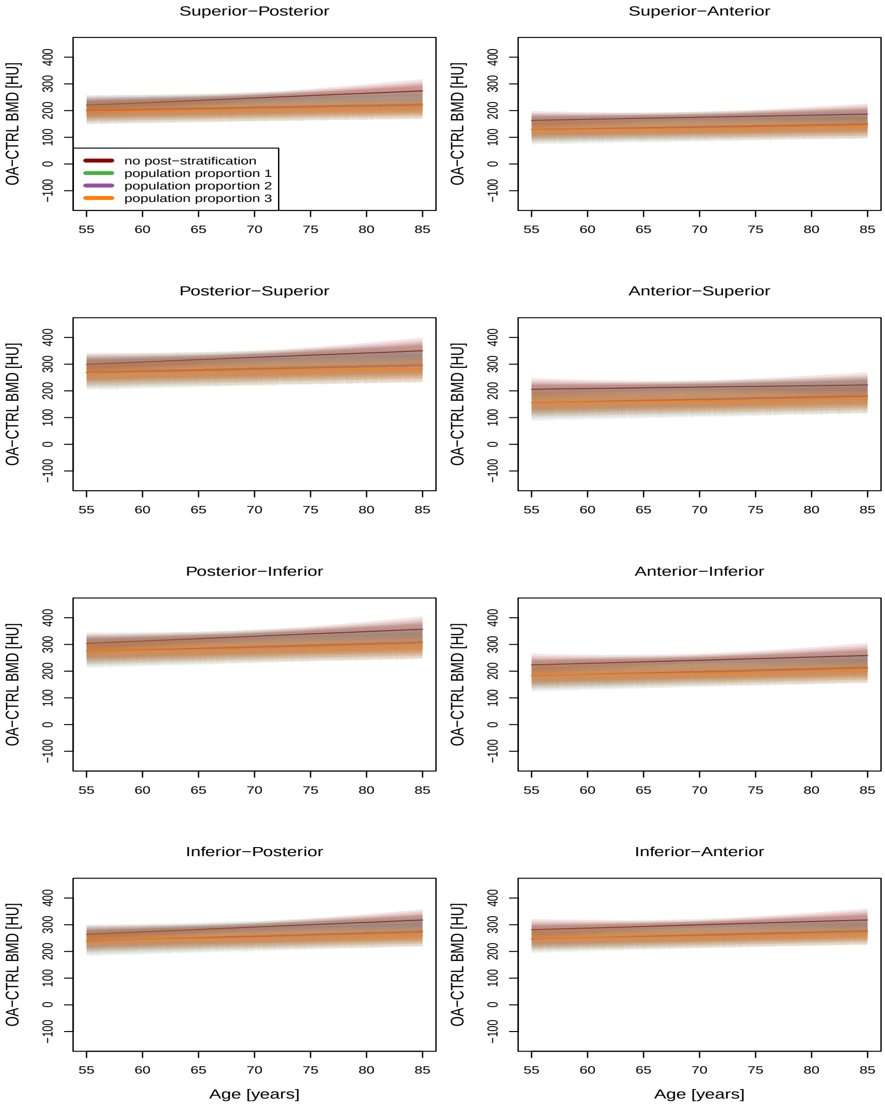
Superior−Posterior
Superior−Anterior
Posterior−Superior
Anterior−Superior
Posterior−Inferior
Anterior−Inferior
Inferior−Posterior
Inferior−Anterior
OA−CTRL BMD [HU]
Age [years]
no post−stratification
population proportion 1
population proportion 2
population proportion 3
-100
0
100
200
300
400
55
60
65
70
75
80
85

(a)

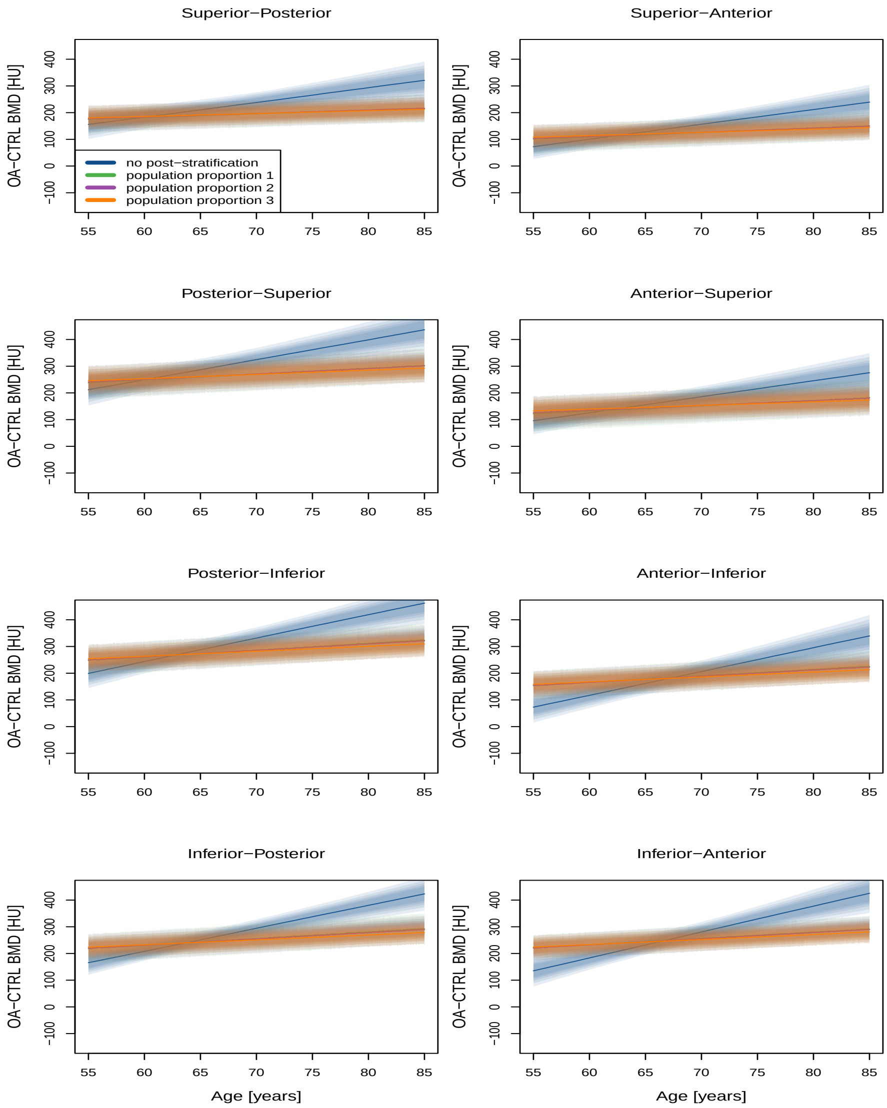

(b)

Fig. A15: Difference of BMD in ST between OA and CTRL vs age, while keeping BMI at 25 kg/m^2, for female (a) and male (b), and the 8 locations. The four colors represent estimated values without post-stratification, and with three different population distributions. The colored surface corresponds to the 89% compatibility interval.

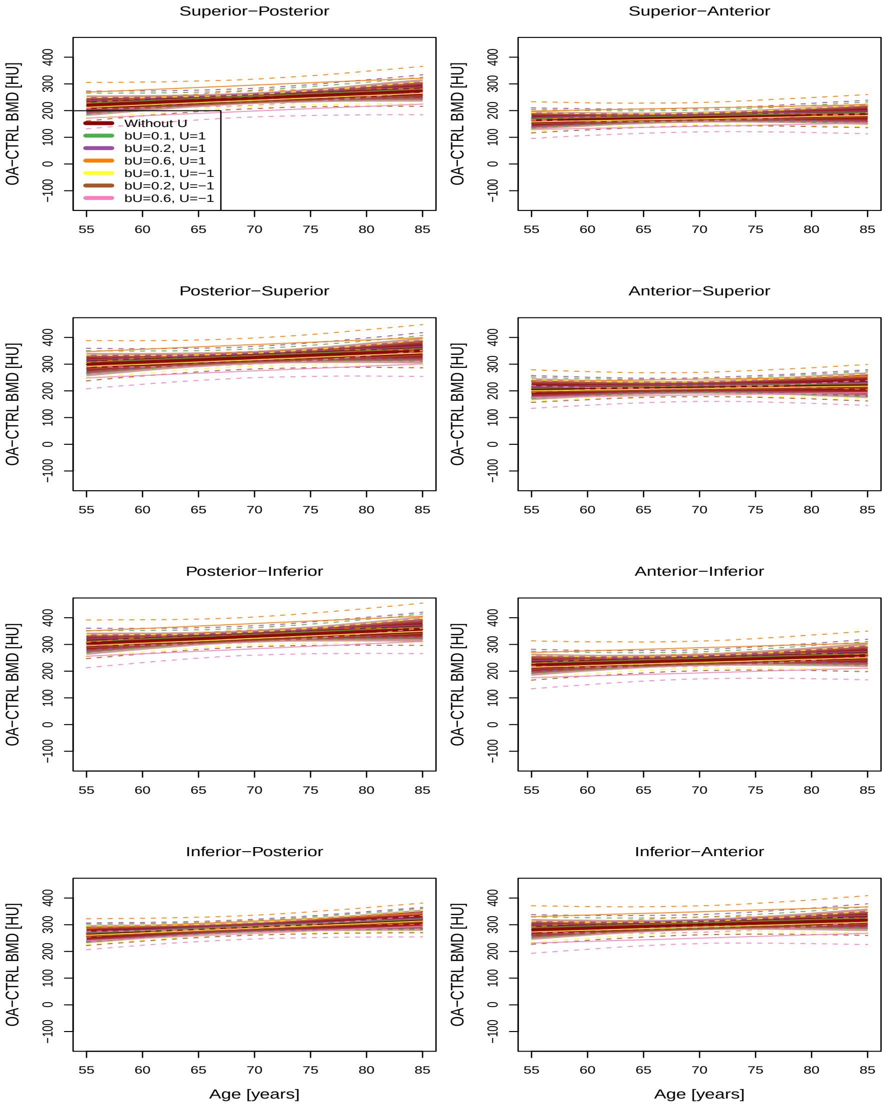

Superior−Posterior
Superior−Anterior
Posterior−Superior
Anterior−Superior
Posterior−Inferior
Anterior−Inferior
Inferior−Posterior
Inferior−Anterior
OA−CTRL BMD [HU]
Age [years]
Without U
bU=0.1, U=1
bU=0.2, U=1
bU=0.6, U=1
bU=0.1, U=−1
bU=0.2, U=−1
bU=0.6, U=−1

(a)

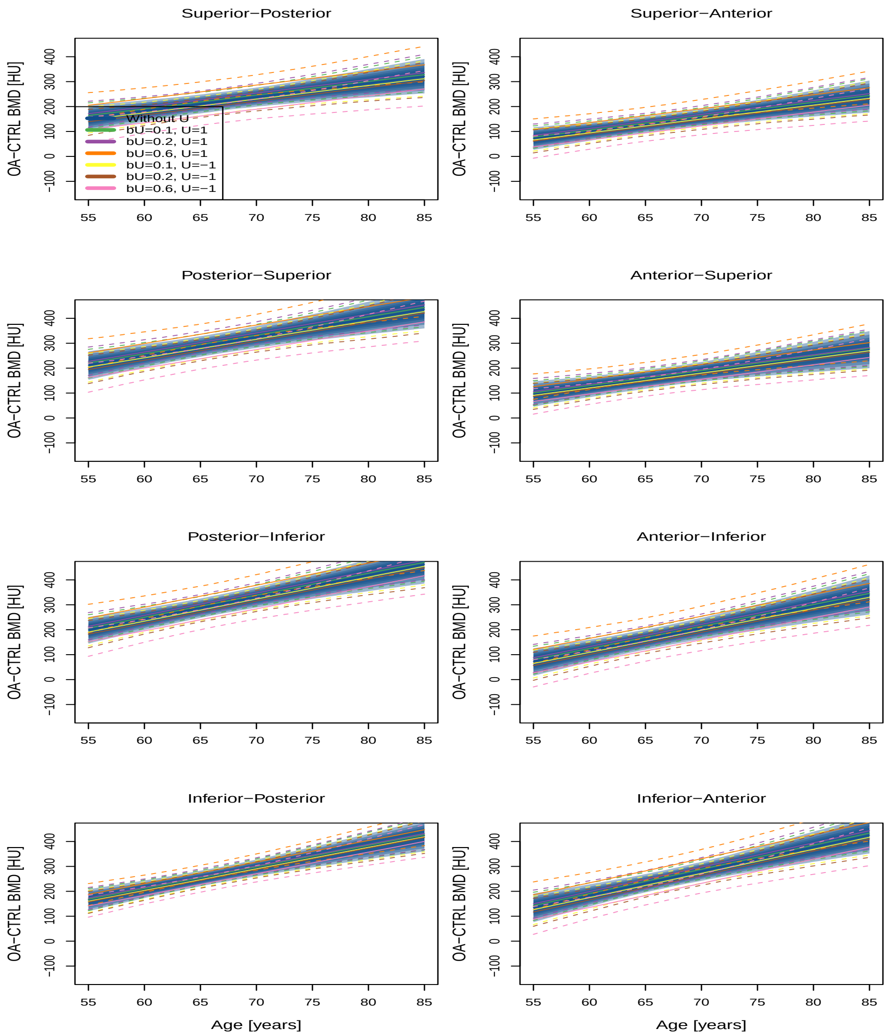

(b)

Fig. A16: Difference in BMD in ST between OA and CTRL versus age, with BMI fixed at 25 kg/m^2, for females (a) and males (b) across the 8 locations. The colored surface represents the estimated values without the presence of an unobserved confounder (U). The six colored solid lines (median) and dashed lines (89% compatibility intervals) represent the estimated values under the assumption that the unobserved confounder U exists. The six colors correspond to three values for the strength of the effect of U (b_U) on glenoid BMD and two levels of U (-1 and +1 z-scores).

1.10 Tables

Sex	Location	50 years	60 years	70 years	80 years	90 years
Female	Superior-Anterior	159.4 [117, 204]	167.6 [139.9, 194.7]	174.9 [154.1, 197.2]	182.7 [150.7, 214.9]	190.4 [141.1, 240]
	Anterior-Superior	201.3 [150.9, 257.5]	207.3 [173.8, 242.3]	212.6 [186, 237.9]	217.5 [179.9, 254.8]	222.4 [162.8, 279.9]
	Anterior-Inferior	212.8 [164.2, 265.8]	225.2 [194.7, 258.6]	237.4 [215.1, 261.2]	249.3 [215, 285.6]	261.7 [207.6, 317.5]
	Inferior-Anterior	274.3 [225.4, 325.1]	286.9 [257.2, 317.7]	299.2 [278.9, 320.6]	311.6 [279.9, 344.8]	323.9 [272, 377.9]
	Inferior-Posterior	255.6 [213.6, 299.8]	272.9 [246.2, 300.2]	290.3 [270, 312.6]	308.4 [276.8, 340.2]	326.1 [276.6, 376.2]
	Posterior-Inferior	298.7 [243.4, 353.2]	316 [283.7, 350.2]	333.9 [311.3, 358.3]	351.7 [316.7, 389.3]	369.2 [313, 429.2]
	Posterior-Superior	294.6 [239.7, 346.7]	311.5 [276.4, 343.3]	328 [303.6, 352.6]	344.4 [307.7, 381.7]	361.8 [304.4, 421.3]
	Superior-Posterior	214.9 [161.4, 259.7]	231.9 [200.4, 260.8]	250 [227.3, 271]	268 [235.7, 303.2]	285.4 [235.4, 342.5]
Male	Superior-Anterior	43.6 [-14.3, 99.3]	99.5 [61.2, 135.7]	155.9 [119.5, 190.8]	211.9 [158.5, 266.6]	267.5 [190.2, 349.7]
	Anterior-Superior	66 [1.1, 131.1]	125.1 [81.4, 167.2]	184.3 [142.5, 223.1]	243.1 [182, 302.6]	303 [212.3, 392.1]
	Anterior-Inferior	26.4 [-47, 92.4]	114 [66.2, 157.8]	202.7 [160, 245]	291.9 [229.2, 354.3]	379.8 [290.1, 475.8]
	Inferior-Anterior	86.9 [9.8, 154.9]	182.8 [137, 226]	279.9 [241.4, 317.8]	376.7 [318.1, 439.3]	473.1 [385.8, 570.4]
	Inferior-Posterior	121.7 [63.6, 175.8]	207 [171, 244.1]	293.6 [260.5, 328.8]	380.4 [329, 433.6]	467.1 [390.6, 546.3]
	Posterior-Inferior	159.7 [86.9, 229.5]	246 [199.6, 293.6]	334.5 [291.7, 377]	423.4 [358.9, 486.5]	510.7 [418.7, 605.5]
	Posterior-Superior	177.6 [105.5, 247.6]	251.3 [205.7, 299.3]	327.2 [284.7, 372.3]	403.2 [337.5, 467.8]	479 [383.1, 576]
	Superior-Posterior	133.6 [64, 194.9]	186.8 [141.7, 228.5]	241.1 [202.7, 281.4]	295.6 [240.1, 356.3]	349.9 [267.6, 439.6]

Sex	Location	50 years	60 years	70 years	80 years	90 years
Female	Superior-Anterior	64.8 [-4.9, 119.4]	110.3 [70.3, 143.3]	156.3 [131.6, 179.7]	203.1 [164.3, 243.7]	249.6 [186.7, 320.2]
	Anterior-Superior	-2.8 [-74.7, 56.5]	48.2 [5.3, 84.3]	100.1 [72, 125.9]	152.7 [108.5, 196.3]	205.3 [135.1, 278.7]
	Anterior-Inferior	-67.7 [-136.9, -12.6]	-11.4 [-53.3, 21.6]	44.8 [20, 67.6]	101.4 [65.6, 139.8]	159 [100.2, 224.3]
	Inferior-Anterior	-85.4 [-133.9, -42.8]	-39.7 [-70.3, -14.2]	5.7 [-14.2, 24.5]	51.4 [21.6, 82]	97.3 [48.9, 147]
	Inferior-Posterior	-109.8 [-165.5, -63.6]	-58.7 [-92.5, -30.5]	-7.4 [-30, 15.4]	44.9 [9.5, 80.6]	97 [40, 154.1]
	Posterior-Inferior	-73.4 [-152.5, -5.7]	-12.3 [-58.4, 26.9]	48.9 [21.4, 74.1]	110.4 [67.1, 155.2]	171.7 [98.5, 248.8]
	Posterior-Superior	57.3 [-30.9, 130.8]	107.9 [57.9, 152.5]	160.4 [131.6, 187.7]	212.9 [166.9, 259.8]	265.5 [186.9, 348.2]
	Superior-Posterior	135.5 [58, 197.5]	174.8 [129.8, 212.2]	214.4 [189.6, 238.7]	255.6 [213.6, 297.3]	295.8 [226.7, 368.6]
Male	Superior-Anterior	42.7 [-1.4, 89.8]	81 [49.1, 109.5]	118.7 [90.2, 143.9]	156 [116, 193.5]	193.9 [135.4, 249.6]
	Anterior-Superior	-40.6 [-89.4, 2.6]	8.6 [-24.2, 37.6]	57.7 [28.1, 86.6]	107.8 [64.1, 152.2]	157.7 [93.8, 223.9]
	Anterior-Inferior	-80.8 [-124.5, -39.6]	-25.4 [-53.2, 3.6]	31.3 [6.3, 57.1]	87.9 [50, 126.6]	143.9 [88.5, 202]
	Inferior-Anterior	-110.4 [-145.8, -78.5]	-56.8 [-78.7, -35.2]	-2.7 [-22.3, 18.9]	52.1 [20.5, 84.9]	106.3 [60.4, 155.4]
	Inferior-Posterior	-127.4 [-166.4, -92.6]	-68.9 [-93.5, -44.3]	-9.6 [-31.8, 15.9]	51 [15.2, 87.8]	110.7 [57.6, 163.9]
	Posterior-Inferior	-84.6 [-136.3, -35]	-24.8 [-59.6, 6.7]	34.9 [5.4, 63.8]	94.8 [50.4, 139.2]	155 [90.2, 221.5]
	Posterior-Superior	19.7 [-39.3, 74.6]	69.2 [28.6, 104.8]	119.5 [83.8, 149.5]	168.3 [118.3, 217.3]	218.2 [146.3, 291.7]
	Superior-Posterior	104.3 [53.2, 154.8]	133.5 [93.5, 166]	162.4 [125.1, 190]	190.4 [142.2, 231.4]	218.6 [153, 278.3]

Sex	Location	17 kg/m2	22 kg/m2	27 kg/m2	32 kg/m2
Female	Superior-Anterior	169.1 [138, 200.2]	170.5 [146.7, 194.2]	171.7 [149.1, 194.3]	173.3 [144.9, 201.2]
	Anterior-Superior	199.8 [157.8, 238.9]	206.3 [175.8, 235.6]	212.8 [185, 240.7]	219.1 [184.7, 255.4]
	Anterior-Inferior	214 [171.3, 252.9]	224.8 [196.3, 253]	235.8 [211.8, 262]	247.2 [215.8, 282.6]
	Inferior-Anterior	280.5 [243, 315.3]	288.3 [262.3, 313.8]	296.2 [273.1, 320.2]	303.8 [274.1, 335.8]
	Inferior-Posterior	283 [253.3, 313.8]	282.1 [259.5, 306.9]	281.8 [259.7, 304.3]	280.9 [253.4, 308.3]
	Posterior-Inferior	334.6 [298.3, 375.3]	328.8 [301.4, 358.1]	322.9 [297.5, 348.8]	317.1 [283.2, 349.2]
	Posterior-Superior	327.1 [288.7, 369.6]	322.8 [293.2, 351.7]	317.8 [290.2, 343.1]	312.5 [277.7, 344.7]
	Superior-Posterior	251.7 [216.6, 287.9]	245.2 [218.3, 270.2]	238.2 [213.6, 262.1]	231.5 [198.9, 262.7]
Male	Superior-Anterior	129 [88.5, 167.7]	128.5 [92.4, 162.4]	127.9 [93.6, 159.5]	127.5 [90.9, 161.5]
	Anterior-Superior	170.8 [123.2, 215.9]	160.9 [120, 200]	151.4 [112.6, 188]	141.2 [100.1, 180.7]
	Anterior-Inferior	168.3 [121.6, 215.7]	162.5 [120.1, 203.8]	156.4 [115.4, 195]	149.7 [106.9, 189.2]
	Inferior-Anterior	239.4 [197, 280.9]	234.5 [195.7, 272.2]	230 [191.7, 266.4]	224.5 [184.8, 263.5]
	Inferior-Posterior	251.6 [215.5, 289.9]	251.2 [218, 284.9]	250.7 [218.6, 282.9]	249.8 [216.3, 283.2]
	Posterior-Inferior	297.4 [250.3, 344.6]	293.2 [250.8, 335.1]	289.4 [247.8, 330.2]	284.7 [242.1, 328]
	Posterior-Superior	297.6 [251.1, 345.9]	292.8 [250.9, 336.4]	288 [248.3, 330.9]	283.5 [241.2, 328.8]
	Superior-Posterior	223.1 [179.5, 267.3]	217.3 [178.9, 256.5]	211.8 [174.3, 249.1]	206.5 [166.6, 245.9]

Sex	Location	17 kg/m2	22 kg/m2	27 kg/m2	32 kg/m2
Female	Superior-Anterior	130.8 [88.9, 165.9]	132 [100.5, 159.7]	133.8 [104.9, 160.9]	134.7 [100.3, 172.4]
	Anterior-Superior	78.4 [36.1, 118.7]	75.6 [42.8, 105.5]	72.9 [40.3, 101.1]	70.1 [29.5, 106.9]
	Anterior-Inferior	19.3 [-23.2, 54.6]	17.8 [-14.3, 44.4]	16 [-14.3, 42.3]	13.4 [-21.1, 48.5]
	Inferior-Anterior	-14.7 [-45.9, 13.5]	-15.9 [-40.6, 5.8]	-17.2 [-40.4, 2.8]	-18.8 [-46.4, 6.9]
	Inferior-Posterior	-34.4 [-66.9, -3.9]	-33.5 [-59.9, -8.8]	-32.5 [-58.3, -8.8]	-32 [-63.2, -1.1]
	Posterior-Inferior	11 [-41.6, 48.8]	14.8 [-20.2, 45.6]	20.7 [-13, 50.7]	25.3 [-15.5, 71.9]
	Posterior-Superior	130.4 [75.9, 173.3]	132.8 [93.8, 166.1]	135.5 [100.2, 169.6]	137.2 [94.2, 188]
	Superior-Posterior	190.4 [136.1, 230.5]	192.6 [157.1, 223.8]	195.6 [164.6, 226.2]	197.4 [159, 246]
Male	Superior-Anterior	109.8 [70.5, 158.9]	104.3 [73, 133.6]	96.9 [68.7, 121.9]	91.3 [46.9, 122.9]
	Anterior-Superior	57.5 [16.5, 112.3]	43.1 [12.2, 76.3]	26.6 [-2.5, 53.4]	11 [-36.2, 45.6]
	Anterior-Inferior	19.8 [-17.8, 64.6]	9.8 [-17.2, 39.4]	-1.1 [-26.3, 23.8]	-11.1 [-49.5, 21.2]
	Inferior-Anterior	-19.9 [-49, 12.5]	-25.8 [-46.6, -3.2]	-32.3 [-50.2, -11.5]	-37.9 [-63.7, -11.9]
	Inferior-Posterior	-36.4 [-68.5, -0.2]	-38.1 [-60.9, -12.3]	-39.9 [-60.4, -16.6]	-41.7 [-69.9, -11.9]
	Posterior-Inferior	15.4 [-26.2, 62.9]	9.4 [-22.2, 41.5]	2.5 [-27.3, 31.1]	-4.1 [-48.3, 34.3]
	Posterior-Superior	106.2 [56.4, 161.5]	99 [60.4, 135.7]	91.1 [54.6, 123.2]	83.4 [31.9, 125.4]
	Superior-Posterior	165.8 [119.1, 221.3]	155.5 [116.7, 189.1]	143.3 [104.8, 171.1]	131.4 [79.2, 168.2]

Sex	Location	50 years	60 years	70 years	80 years	90 years
Female	Superior-Anterior	268.2 [241.9, 295.3]	246 [226.7, 265.3]	223.4 [203.7, 242.7]	200.9 [174.3, 227.3]	178.4 [141.5, 214.4]
	Anterior-Superior	293.5 [262.9, 324.6]	264.2 [241, 287.5]	234.4 [210.7, 258.4]	204.6 [171, 236.5]	174.5 [128.5, 218.6]
	Anterior-Inferior	307.2 [281.4, 334.5]	274.3 [255.1, 294.3]	241.3 [221.3, 260.9]	208.2 [180.7, 234.2]	174.9 [137, 210.5]
	Inferior-Anterior	279.5 [256.4, 302.7]	247.6 [230.8, 264.2]	215.6 [198.5, 232.3]	183.5 [158.8, 207.5]	151.4 [117.2, 184.7]
	Inferior-Posterior	288 [261, 315.6]	253 [232.8, 272.5]	217.4 [197.2, 237]	181.5 [154.1, 209.4]	146 [107.9, 184]
	Posterior-Inferior	346.9 [319.7, 375.3]	312.8 [292.8, 332.8]	278.5 [257.7, 298.4]	244.1 [215.4, 271.8]	209.6 [169.3, 249]
	Posterior-Superior	353.4 [322.5, 382.9]	325.2 [303.2, 347.1]	297.2 [275.7, 319]	268.8 [239.3, 299.2]	241.1 [200.2, 281.9]
	Superior-Posterior	320.9 [297.6, 344.9]	301.7 [284.1, 320.1]	282.4 [264.7, 300.2]	263.1 [238.5, 287.9]	243.6 [208.7, 277.9]
Male	Superior-Anterior	338.3 [315.4, 360.7]	299.4 [284.7, 313.6]	259.9 [242.3, 277]	220.5 [191.8, 248]	180.8 [139.6, 221.5]
	Anterior-Superior	375.8 [347.2, 404.5]	327.9 [309.3, 345.9]	279 [257.7, 301.1]	230.3 [195.8, 265.6]	182.1 [130.6, 233.1]
	Anterior-Inferior	373.1 [349.9, 397.2]	316.9 [302, 331.8]	260.3 [242, 278.7]	203.8 [173.8, 233.3]	146.8 [103.1, 189.5]
	Inferior-Anterior	336.1 [316.2, 356.3]	282.9 [270.2, 295.7]	229.4 [213.4, 244.9]	175.6 [149.5, 201.5]	122.3 [83.9, 159.8]
	Inferior-Posterior	341.7 [317.5, 365.2]	282.9 [267.6, 297.7]	223.5 [205.1, 242.1]	164.6 [134.1, 194.7]	105 [60.8, 149.2]
	Posterior-Inferior	414 [388.4, 439.3]	354.4 [338.1, 370]	294.5 [275.6, 313.2]	234.4 [203.6, 265.4]	174 [129.5, 219.8]
	Posterior-Superior	436.7 [410.5, 464]	387.6 [370.2, 404.4]	337.4 [317.3, 357.7]	286.9 [254.6, 320.1]	236.9 [190.5, 285.3]
	Superior-Posterior	391.5 [370, 413.3]	361.5 [348.1, 375]	331.2 [314.6, 347.9]	301.2 [273.8, 328.8]	271 [230.4, 311]

Sex	Location	50 years	60 years	70 years	80 years	90 years
Female	Superior-Anterior	428 [387.9, 469.9]	413.5 [389.2, 437.2]	398.7 [384.7, 411.3]	383.6 [361.6, 405]	369.2 [329.5, 405.5]
	Anterior-Superior	494.8 [450.4, 546.8]	471 [444.3, 500.5]	446.8 [431.6, 461.1]	422.2 [396.6, 445.3]	398.3 [351.3, 438.2]
	Anterior-Inferior	520.5 [475, 569.9]	499.7 [472.7, 529.1]	478.6 [463.6, 495.3]	457.6 [432.3, 482.8]	436.9 [390.8, 479.6]
	Inferior-Anterior	553.9 [507.9, 602.4]	534.5 [507.1, 563.2]	514.6 [500.7, 530.4]	495.5 [470, 520.2]	476 [430.7, 519.9]
	Inferior-Posterior	542.7 [506.7, 584]	525.7 [504.4, 548.9]	508 [496.6, 520.1]	490 [469.8, 510]	472.7 [436.2, 507.5]
	Posterior-Inferior	645.7 [594.8, 697.2]	629 [599.9, 659.1]	612.5 [597.4, 628.7]	595.8 [570.5, 622.8]	578.6 [533.9, 627.3]
	Posterior-Superior	647 [596, 696.6]	636.4 [606.1, 665.7]	625.4 [608, 641.3]	614.3 [586.7, 640.7]	603.3 [555.6, 649.8]
	Superior-Posterior	535.6 [483.8, 579.4]	534 [503.4, 560.4]	532.9 [515.8, 547.1]	531.3 [507, 556.5]	529.3 [488.6, 576.2]
Male	Superior-Anterior	382.4 [328.7, 431.1]	398.8 [361.6, 433.5]	415.7 [383, 446.4]	432.4 [389.8, 475.1]	448.7 [390.4, 509.8]
	Anterior-Superior	441.7 [384.2, 499.5]	452.2 [412.5, 493]	463.2 [429.9, 495.9]	473.9 [429.2, 518.2]	484.9 [420, 549.3]
	Anterior-Inferior	398.5 [333, 458.9]	430.7 [384.9, 472.4]	463.7 [423.2, 499.7]	495.3 [444.1, 547]	526.6 [456.5, 604.4]
	Inferior-Anterior	423.7 [350.1, 486.3]	465.7 [420.7, 506.6]	509.5 [473.8, 542.8]	552.9 [503.8, 604.8]	595.8 [523.9, 678.1]
	Inferior-Posterior	463.2 [411.9, 510.6]	489.8 [456.1, 523.2]	517.7 [489.4, 545.5]	544.6 [506.9, 584.8]	572 [517.7, 631.9]
	Posterior-Inferior	572.8 [507.2, 637.4]	600.5 [555.3, 644.9]	629 [590.2, 667.6]	656.9 [606.6, 709]	684.7 [613.7, 759.4]
	Posterior-Superior	614.3 [548, 678.6]	638.9 [594.5, 685.9]	664 [627.1, 705.2]	690 [640, 744.9]	714.8 [644.1, 792.4]
	Superior-Posterior	524.7 [461.2, 582.2]	548.1 [505.6, 589.1]	572.5 [537.4, 609.6]	597.1 [551.4, 647.1]	621.3 [556.8, 694.5]

Sex	Location	50 years	60 years	70 years	80 years	90 years
Female	Superior-Anterior	333 [268.3, 383.4]	356.4 [318, 385.8]	380 [360.4, 396.4]	403.7 [376, 435]	426.7 [379.4, 485.2]
	Anterior-Superior	292.2 [225.3, 341.3]	313.6 [273.3, 341.8]	334.7 [314.2, 350.1]	356.4 [328, 387.2]	377.5 [329.8, 436.6]
	Anterior-Inferior	240.3 [174.1, 287.6]	263.4 [223.1, 291]	286.8 [266.5, 301]	309.5 [284.4, 337.8]	332.7 [288.3, 385.7]
	Inferior-Anterior	194.5 [148.9, 230.9]	208.2 [180.1, 229.2]	222 [206.4, 232.3]	234.8 [215.7, 255.3]	248.5 [214.8, 285.2]
	Inferior-Posterior	177.7 [129.1, 219.5]	194.1 [163.8, 218.3]	210.6 [194.6, 222.9]	226.6 [205, 248.8]	242.4 [203.9, 285]
	Posterior-Inferior	274 [198.6, 337.1]	301 [257.3, 337.3]	327.6 [304.6, 345.9]	353.9 [321.9, 388.9]	380.5 [323.1, 445.3]
	Posterior-Superior	410.1 [325.2, 478.1]	433.9 [385.3, 473.4]	457.7 [433.7, 479.5]	481.9 [444.3, 520.6]	505.7 [440.2, 576.3]
	Superior-Posterior	456.5 [384.6, 515.8]	476.3 [434, 512.5]	497 [475.8, 516.3]	517.9 [485.8, 550.9]	538.1 [482.5, 602]
Male	Superior-Anterior	381 [339.8, 427.8]	380.2 [348.3, 408.8]	379.2 [352, 398.6]	377.3 [345.2, 402.7]	376.2 [331, 411.7]
	Anterior-Superior	335.7 [292.1, 372.7]	336.1 [305.9, 363.8]	337.2 [314.1, 358.5]	338 [311.6, 366.3]	338.7 [303.3, 380.7]
	Anterior-Inferior	291.7 [253, 331.4]	291.6 [264.6, 319.7]	291.2 [271.6, 313.4]	291.3 [267, 317.7]	291.2 [254.6, 328.6]
	Inferior-Anterior	225.7 [194.3, 254.1]	225.8 [206, 247.1]	226.2 [213, 243.6]	227.1 [210.7, 249.1]	227.5 [203.2, 258.9]
	Inferior-Posterior	213.3 [180.8, 245.6]	213.7 [192.2, 237.2]	213.9 [198.5, 233]	214.5 [194.7, 238.7]	215.1 [186.7, 250.1]
	Posterior-Inferior	329.3 [280.6, 378.3]	329.1 [294.8, 362.8]	329.5 [303.3, 354.1]	329.4 [297, 361.7]	329.6 [283.1, 377.1]
	Posterior-Superior	456.3 [399.2, 508.9]	456.7 [415.5, 491.9]	456.9 [424.5, 483.3]	456.4 [417.2, 491.2]	456.8 [401, 508.4]
	Superior-Posterior	495 [446.6, 546.7]	494.8 [455.3, 528.6]	494.1 [459.3, 518.4]	492 [452.9, 522.4]	491 [436.7, 531.8]

References

[1] Vehtari, A., Gelman, A., Gabry, J.: Practical bayesian model evaluation using leave-one-out cross-validation and waic. Statistics and computing **27**, 1413–1432 (2017)

[2] Watanabe, S., Opper, M.: Asymptotic equivalence of bayes cross validation and widely applicable information criterion in singular learning theory. Journal of machine learning research **11**(12) (2010)

[3] Gabry, J., Simpson, D., Vehtari, A., Betancourt, M., Gelman, A.: Visualization in bayesian workflow. Journal of the Royal Statistical Society Series A: Statistics in Society **182**(2), 389–402 (2019)

[4] Kennedy, L., Gelman, A.: Know your population and know your model: Using model-based regression and poststratification to generalize findings beyond the observed sample. Psychological methods **26**(5), 547 (2021)